Exploration of Molecular Machinery Affected by Cerium Oxide Nanoparticles in Benzene Induced Leukemia

by

Asiya Essa

Department of Biochemistry
Faculty of Biological Sciences
Quaid-i-Azam University
Islamabad, Pakistan

2019

Exploration of Molecular Machinery Affected by Cerium Oxide Nanoparticles in Benzene Induced Leukemia

A thesis submitted in partial fulfillment of the requirements for the

Degree of Master of Philosophy in

Biochemistry/ Molecular Biology

by

Asiya Essa

Department of Biochemistry

Faculty of Biological Sciences

Quaid-i-Azam University

Islamabad, Pakistan

2019

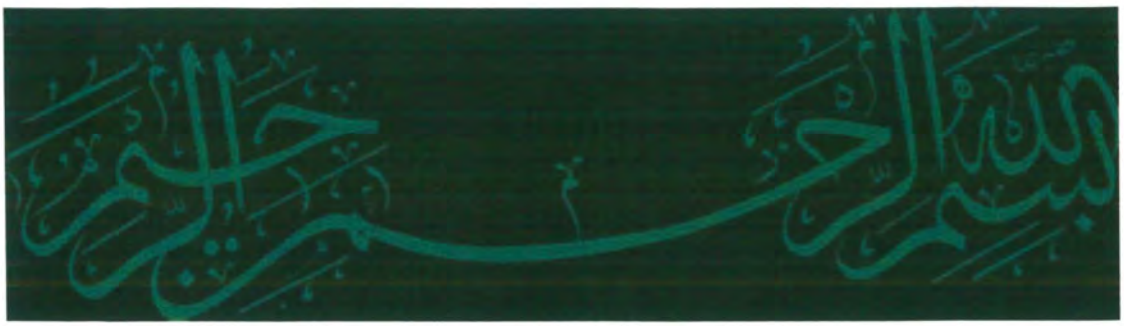

In the Name of ALLAH, the Most Gracious, the Most Merciful.

Declaration

I hereby declare that this research study represents my own efforts and hard work. The thesis is written and composed by me. No part of this work has been presented previously for any other degree or certificate.

Asiya Essa

CERTIFICATE

This thesis, submitted by **Ms. Asiya Essa** to the Department of Biochemistry, Faculty of Biological Sciences, Quaid-i-Azam University, Islamabad, Pakistan, is accepted in its present form as satisfying the thesis requirement for the Degree of Master of Philosophy in Biochemistry/Molecular Biology.

Supervisor:

Dr. Mariam Anees
Associate Professor

External Examinar:

Dr. Zubair Anjum
Assistant Professor
Department of Zoology,
PMAS Arid Agriculture University, Rawalpindi

Chairperson:

Dr. Muhammad Rashid Khan
Professor

Dated: November 06, 2019

Table of Contents

Acknowledgements

All praises and glories be to **Almighty Allah** the lord of the universe for **His** infinite mercy upon us, whomever **He** guides shall never go astray and whomever **He** allows to astray shall never find the guidance. May the peace and blessings of Allah be upon His noble **Prophet (PBUH)**and upon his companions.

I am greatly honored to pay my gratitude to my respected supervisor **Dr. Mariam Anees** whose inspiring guidance, valuable suggestions, immense patience and encouragement made me achieve this goal of my life.

I am thankful to **Prof. Dr. Muhammad Rashid Khan**, Chairperson, Department of Biochemistry, for providing us a healthy research environment. I am thankful to all respected teachers who taught me and made me able to achieve this milestone of my life.

I would like to thank my **Family** for their support, help and care. My siblings helped me in every single way beyond imagination. I would like to pay heartily gratitude to my brother in law **Faisal Iqbal** and Cousin **M.Tariq.**

I would like to pay my immense gratitude to all those seniors who guided me, supported me and helped me whenever I needed them specially **Sidra Bukhari, M. Hamid Siddique** and **Inam Banochi** for their cooperation, suggestions and nice company during my research work which is precious to me in all regards. Without their help and cooperation my research would have been really difficult. I would like to acknowledge the cooperative attitude of PhD seniors **Ayesha Ishtiaq** and **Zain Ali**. I am also very thankful to my batch mates **Faisal Abbasi, Durdana** and **Banafsha** for their cooperation.

I present heartiest thanks to my dear friend **Shaheen** for supporting and encouraging me throughout my research work.

I convey my heartiest thanks to the departmental clerical staff especially **Mr. Fayyaz, Mr. Tariq, Mr. Shahzad** and **Mr. Masood** for their services towards students.

Asiya Essa

List of Figures

List of Tables

List of Abbreviations

Abs	Absorbance
ALP	Alkaline Phosphatase
ALT	Alanine Transferase
AML	Acute Myeloid Leukemia
B	Benzene
CNTs	Carbon Nanotubes
EDTA	Ethylene Diamine Tetra Acetic Acid
FTIR	Fourier Transform Infrared Spectroscopy
FWHM	Full Width at Half Maximum
mg/dl	Milligrams per deciliter
NM	Nano-medicine
RBCs	Red blood cells
ROS	Reactive oxygen species
U/min	Unit per minute
WBCs	White blood cells
XRD	X-ray Diffraction Spectroscopy

Abstract

Cancer is considered as one of the most lethal diseases despite the advancement in therapeutics. Acute myeloid leukemia (AML) occurs when there is massive expansion of abnormally differentiated immature white blood cells that occasionally spread to other body parts. Nanoparticles are being used for therapeutic purpose successfully by serving as a vehicle for targeted drug delivery. Doxorubicin is a known anticancer drug with cytotoxic side effects thus limiting its clinical applications. We designed a study to identify the anticancer potential of cerium oxide (CeO_2) nanoparticles coupled with doxorubicin. Properties of drug loaded nanoparticles were identified by XRD (X-Ray Diffraction) and FTIR (Fourier Transform Infrared Spectroscopy). Rats were divided into five experimental groups and leukemia was induced by giving intra-peritoneal injections of benzene. After different treatments for 24 alternate days, rats were sacrificed and blood samples were collected along with different organs for further analysis. Interestingly, hematological assays showed powerful anti-cancerous activity of cerium oxide. The nanoparticles reduced back the size and subsequent weight of hypertrophic liver, kidney and heart near to the normal. The number of apoptotic cells in each group was characterized by Annexin V assay. The nanoparticles treated group showed reduced levels of ALP, AST and ALT. qRT-PCR was performed to check the expression of selected genes of TRAIL pathway, NF-kappa B pathway, p53 and STMN1. The expression of p53 was found to be down regulated in treated groups. The expression of caspases was found to be up regulated in nanoparticles treated group. To summarize, cerium oxide nanoparticles showed good anti-leukemic activity in vivo. Further studies should be carried out to authentic the role of cerium oxide and develop it as a potential therapeutic drug.

Key Words: Acute Myeloid Leukemia, Cerium oxide nanoparticles, Doxorubicin, Nanomedicine

1. Introduction

1.1. Cancer

Being a devastating proliferative disease, cancer is one of the major causes of death, irrespective of advancements in the field of prevention, diagnosis and treatment (He *et al.*, 2016; Qin *et al.*, 2017; Zhang *et al.*, 2017). One of the major causes of morbidity and mortality around the world is cancer and the figure of the cases are frequently rising and expected to be 21 million by 2030 (DeSantis *et al.*, 2015; Miller *et al.*, 2016). Cancer is a major issue of the society that is affecting all the human ethnicities. Cancer is a diverse syndrome at tissue level and the major issue of cancer is its proper diagnosis that is followed by its specific treatment (Meacham *et al.*, 2013; Siegel *et al.*, 2013).

Changes in cell functions occur by a sequence of consecutive mutations in genes which results in cancer. Chemical compounds also cause mutations in genes leading to cancer (Aizawa *et al.*, 2016). Sometimes, cellular relations are disrupted by cancer which results in the dysfunction of essential genes. Abnormal proliferation occurs due to a disturbance in the cell processes (Cigudosa *et al.*, 2010; Seto *et al.*, 2010).

1.2. Cancer Causes

Multiple factors are involved in inducing cancer and it is not an effect of single mutation. To find out the primary cause of cancer occurrence and progression is almost impossible. Cancer is usually a consequence of changes in genome of transformed cells which generally consist of mutations in DNA of regular cells labeled as mutants (Vogelstein and Kinzler, 2004). Different types of carcinogens or mutagens that may be environmental factors, chemicals and radiations are responsible for causing these mutations (Boyland, 1952).Genotoxic agents cause harm to the hereditary material in a cell, which may direct to cancer causing mutation.

1.3. Cancer Progression Levels

Degradation of extracellular matrix which is achieved by a variety of proteases including the matrix metallo-proteineases is a major step in the way of cancer progression and the establishment of metastasis (Moss *et al.*, 2012; Cui *et al.*, 2017). Cancer appears to grow progressively. Typical cell changes its hereditary make up that actuates cell to be converted into cancerous cell. Before dysplastic stage the cells are hyperplastic, then the nucleus to cytoplasmic ratio gets increased marking their

transition from hyperplastic to dysplastic and finally becomes neoplastic. Neoplastic cells have the capacity to attack surrounding tissues and become metastatic and invade blood vessels and spread all over the body. Figure 1.1 shows the different steps of progression of cancer cells.

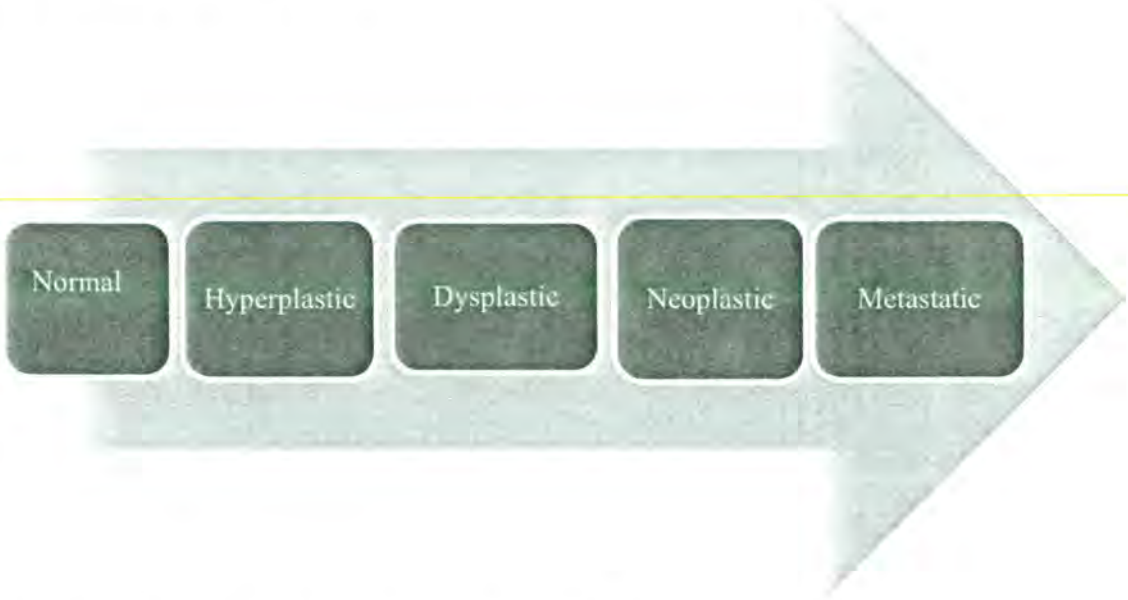

Figure 1.1: Flow diagram of cancer progression

1.4. Hallmarks of Cancer

The hallmarks of cancer comprise of six essential natural abilities created through the progression of cancer. The hallmark includes increased resistance to cell death, evasion of growth suppressors, gain of replicative immortality, gain of cell survival signaling, increased angiogenesis and increased invasive potential of cells. These competencies rise because of different mutations in charge of creating genetic diversity and genome. There is addition of four further developing hallmarks including genome instability, reprogramming of energy metabolism, tumor promoting inflammation, and evading immune destruction. These hallmarks can turn out to be a pattern to recognize and expand new ways to treat cancer (Hanahan and Weinberg, 2011).

Figure 1.2: Hallmarks of cancer (Hanahan and Weinberg, 2011)

1.5. Leukemia

Leukemia word is originated from two Greek words leukos meaning white and haima meaning blood. Rudolf Virchow in 1946 first proposed the modern term leukemia. The first pathological and anatomical depiction of leukemia is provided by the famous French physician Alfred Armand Louis Marie Velpeau (Geary, 2000).Leukemia has been characterized into four different types and classification is based upon cellular origin whether it is lymphoid lineage or myeloid; or by the course of the disease if it is acute or chronic. The four types consist of acute myeloid leukemia (AML), chronic myeloid leukemia (CML), acute lymphocytic leukemia (ALL) and chronic lymphocytic leukemia (CLL). They vary essentially in relation to morphological, immune-phenotypic and structural features of malignant cells (Jin *et al.*,2016). Acute myeloid leukemia (AML) is described by clonal increase of abnormally differentiated immature white blood cells of myeloid lineage. Accumulation of blasts or immature white blood cells with impairment of regular haemopoiesis resulting in hemorrhage, anemia and severe infections which results in the proliferation of immature myeloid cells (Ganzel *et al.*, 2016).

Immature blood cells start accumulating in the bone marrow; however, in majority of cases they rapidly build up in the blood and occasionally spread to other regions of

the body like spleen, lymph nodes, liver, central nervous system and testes (Ferrara and Schiffer, 2013). Gilliland in 2001 proposed the two hits model which classified the key oncogenic events. The two hits model theorizes that AML is the result of cooperation between two wide classes of mutations, class 1 mutations that present proliferative and survival advantage and class two mutations that influence the procedure of cell isolation and apoptosis. However, parallel sequencing technologies have recently identified new group of mutations that do not correspond to any of two classes, as a result, they have not been classified although these generally encourage epigenetic modifications (Kelly *et al.*, 2002).

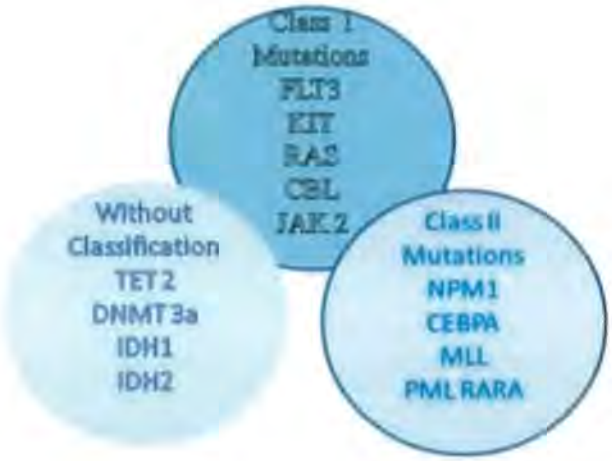

Figure 1.3 Model of cooperation between mutations associated with appearance of AML (Kelly *et al.*, 2012).

1.5.1 Classification of Acute Myeloid Leukemia

In 1976, the French- American-British (FAB) classification initially put forward classification for the AML which subdivides the AML into eight different subtypes according to the reactivity of blasts with histochemical stains and morphological appearance of immature white blood cells (Dohner *et al.*, 2015). Table 1.1 shows FAB classification of acute myeloid leukemia

Table 1.1 FAB Classification of Acute Myeloid Leukemia

M0	AML without differentiation
M1	AML with minimal differentiation
M2	AML with differentiation
M3	Acute promyelocytic leukemia hypergranular or typical
M3v	Acute promyelocytic leukemia hypogranular
M4	Acute myelomonocytic leukemia
M4v	Acute myelomonocytic leukemia with bone marrow eosinophilia
M5	Acute monocytic leukemia
M6	Acute erythroid leukemia
M7	Acute megakaryocytic leukemia

1.5.2 Role of Benzene in AML

Benzene is a broadly used element and is a ubiquitous ecological pollutant (Arnold *et al.*, 2013). It is a carcinogenic compound as well and has the ability to cause leukemia. It is metabolized into toxic metabolites specifically phenolic compounds which comprise of hydroquinone, catechcol and phenol. These compounds change normal cell development and at cellular level cause genetic alteration (Morimoto and Wolff, 1980).

Benzene is in charge of causing acute myeloid leukemia besides other hematopoietic malignancies. It causes leukemia by generating reactive oxygen species which causes genotoxicity of bone marrow cells. Benzene while coming across blood and bone marrow cells, results in structural and genomic damage of bone marrow cells. Benzene and its metabolites cause redox reactions that modify DNA at cellular level (Kolachana *et al.*, 1993).

1.5.3. Diagnosis of Acute Myeloid Leukemia

There are numerous ways to identify Acute Myeloid Leukemia, but frequently it is diagnosed with blood tests. These tests are carried out to check morphology of peripheral blood cells, myeloblasts and bone marrow cells as they change in leukemia. The morphological changes observed are increased nucleus to cytoplasm ratio, reduced cytoplasmic content and distortion in nuclear shape specifically, properties of immature blast cells. When 30% or more cells display such morphology of blast cells in blood then it is considered as Acute Myeloid Leukemia (AML). Due to differentiation in blast cell morphology, AML is subdivided into 9 further types which have been described above (Bennett *et al.*,1976).

For morphological studies, numerous staining procedures can be adopted; however, most preferable one is Giemsa staining. Similarly, acute myeloid leukemia can also be analyzed by genetic analysis of patients, as they acquire non-random chromosomal aberrations (Rowley, 1980). On an individual basis, the therapeutic responses can also be observed. One of the parameter to diagnose AML is the variation in hepatic (ALT, AST & ALP) and renal biomarkers in serum of affected, because of hepatic cytotoxicity by benzene (Egeman and Ferda, 2009). Apoptotic genes' expression gets suppressed while that of cell proliferation genes gets increased in leukemic cells (Shen *et al.*, 1996).

1.6. Treatment

There are different conventional therapies for the treatment of cancer comprising of radiation therapy, chemotherapy, surgery, immunotherapy and hormonal therapy. For treating acute myeloid leukemia, gene and stem cell transplantation is particularly used to improve and increase patient survival up to a few years.

In chemotherapy, numerous anti-cancerous chemotherapeutic agents are utilized to slow down the propagation of cancer cells and carry out the death of cancer cells (Partridge *et al.*, 2001). However, these chemotherapeutic agents are very expensive and have several adverse effects on neighboring normal cells as they are incapable of differentiation between normal and cancer cells (Meisenberg, 2015). In addition to the intended therapeutic effect, chemotherapy can induce immunogenic cell death (Frohlich *et al.*, 2016). Adverse effects of chemotherapy mostly comprise of fatigue, hair loss, nausea, vomiting and diarrhea (Patridge *et al.*, 2001). Despite of the

mentioned side-effects, chemotherapy is frequently being utilized to treat AML for patients of all ages. To increase effectiveness, anticancer drugs are being utilized in combination with other drugs to treat AML.

With increasing age, recurrence free survival becomes less. Targeted therapy is required by AML which targets factors involved in deregulating cellular activities and retaining leukemic state i-e tyrosine kinase over-expression, drug resistance, and enhanced angiogenesis which maintain leukemic state (Schlenk *et al.*, 2008). Recurrence of leukemia can also take place after treatment because of persisting leukemic cells. This state is called as the minimal residual disease (Su *et al.*, 2015).

1.7. Doxorubicin

Doxorubicin is one of the foremost extensively used drug of the fifty or so chemotherapeutical compounds presently in clinical use and has been an important antitumor agent since NCL approval in 1974 (Devita *et al.*, 2012). Doxorubicin consists of two main components, aglycones and sugar moieties and it is also known as anthracycline antibiotic. The non sugar component is comprised of tetracyclic ring having quinine-hydroquinone adjacent groups, and sugar component is attached through glycosidic bond. The chemical name is 3-amino-2, 3, 4-trideoxy-L-fucosyl moiety, according to set rules of Physical and Applied Chemistry (Tacar *et al.*,2013). Its structure is exhibited in figure 1.4

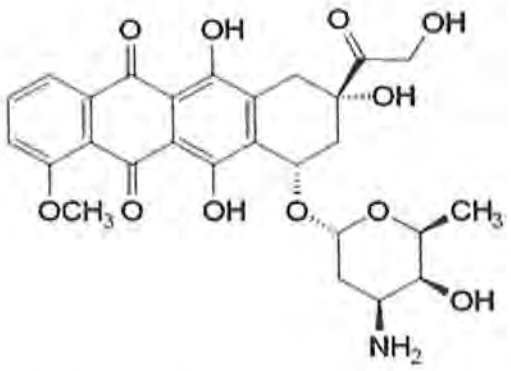

Figure 1.4: Structure of Doxorubicin (Tagmir and Riahi, 2017)

1.7.1. Mode of Action

Doxorubicin binds with high affinity to the DNA by typical intercalation among base pairs as it is quickly taken up into nucleus of the cells (Philips *et al.*, 1988).Once it is

intercalated with DNA, it disturbs the mechanism of topisomerase II enzyme and it disrupts the religation step of the DNA (Larsen *et al.*,2003; Sordet *et al.*,2003; Wilstermann *et al.*,2003).

When anthracyclines or chemotherapeutic drug bind to the DNA, they disrupt its functioning and block the activity of enzyme topoisomerase II and as a result, stimulate DNA damage response pathways which lead to cell death by interrupting cancer growth (Patel and Kaufmann,2012; Sawyer, 2013). Topoisomerase II is an important enzyme that plays a crucial role in DNA transcription and replication and also in chromosome segregation (Pogorelcnik *et al.*, 2013).

Doxorubicin reacts with cell constituents in different ways. Its planer aglycone moiety can embed itself between adjoining DNA base pairs. Doxorubicin causes breaks in single and double stranded DNA. It modifies capacity of nuclear helicases to separate double stranded DNA into single stranded DNA. Like other anthracyclines, doxorubicin can experience reduction in one or two electrons being members of the quinine family and thus produce reactive oxygen species that harm lipid bilayers and other macromolecules. Different signaling pathways are engaged in activating apoptotic cell death by doxorubicin. The p53 and Fas/Fas ligand frameworks are additional pathways utilized for doxorubicin mediated apoptosis in various cell lines (Hande, 2008; Priestman, 2012).

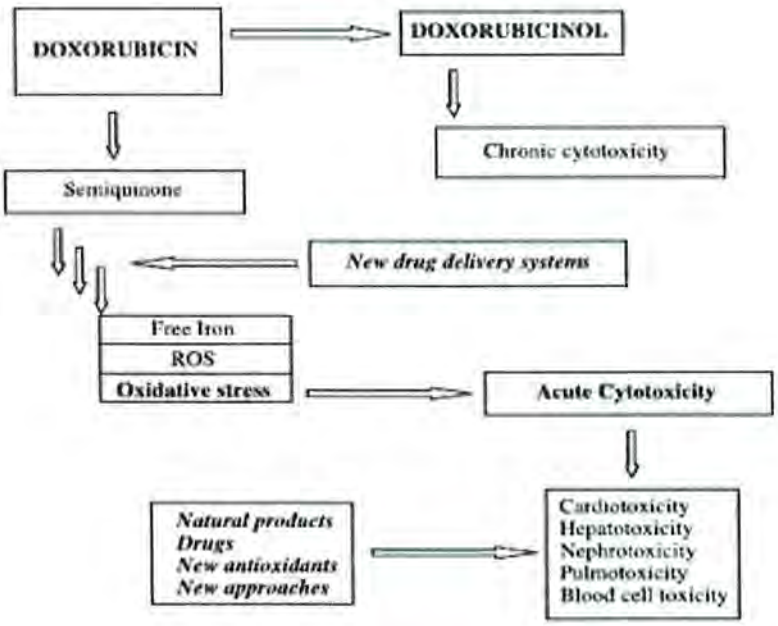

Figure 1.5 Mode of action of doxorubicin (Injac and Strukelj, 2008)

Doxorubicin and other anthracyclines belong to a group of chemotherapeutic drugs with a wide range of activities that are used alone or in combination and are effective against a range of hematological malignancies and solid tumors (Weiss, 1992). The key side-effect of doxorubicin is cardiotoxicity, which takes place both acutely and chronically which limits its clinical application (Cardinale *et al.*, 2010).

The precise mechanism responsible for anthracycline-induced cardiomyopathy and pathogenesis of cardiotoxicity has not been entirely elucidated, even though anthracyclines have been studied for years (Minotti *et al.*,2004; Takemura *et al.*, 2007;Octavia *et al.*, 2012). From the time when the anthracycline was discovered, the primary mechanism capable of its cardiotoxic potential has been credited to the excessive reactive oxygen species generation and a number of ROS dependent methods have been proposed, such as damage to the DNA, mitochondrial dysfunction, intracellular calcium dysregulation and attenuation in protein synthesis (Minotti *et al.*, 2004; Takemura *et al.*,2007; Gianni *et al* 2008). The harmful effects stimulated by doxorubicin are exhibited in figure 1.6.

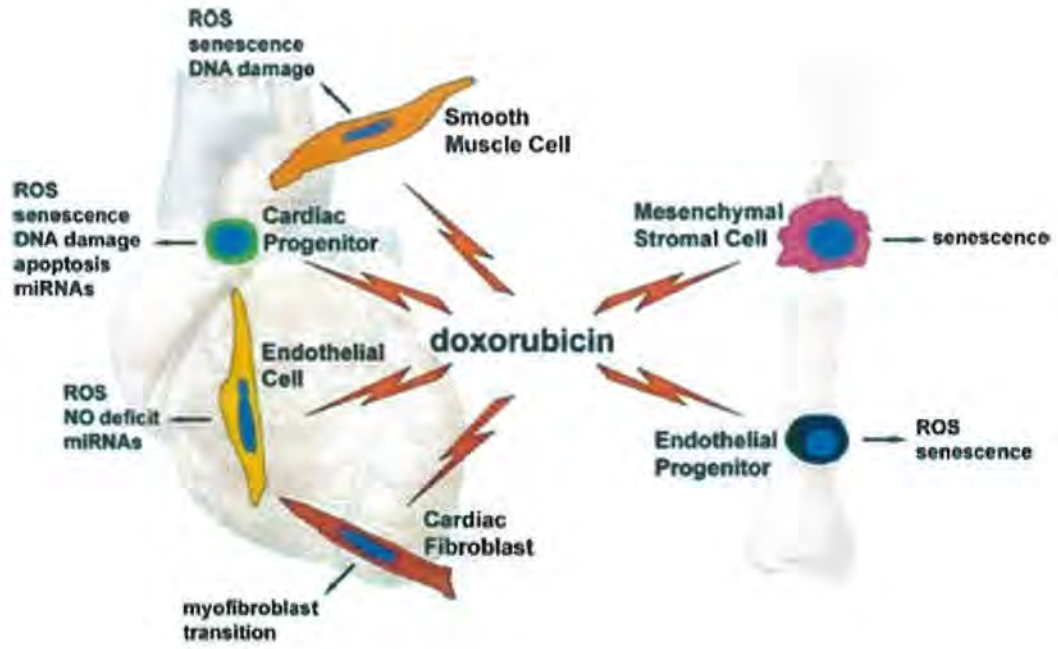

Figure1.6 Harmful effects induced by doxorubicin (Cappetta *et al.*, 2018)

1.8. Drug Delivery System

Drug targeting has come out as one of the latest technologies for the drug delivery (Torchilin, 2000). Drug delivery system based upon engineered nanoparticles gained much importance after numerous decades of technological developments (Amnold *et al., 2015).* Nanoparticles utilized for drug delivery can be easily manufactured from either hard or soft materials and their sizes can be managed in range from 1-100nm and their structures being devised to carry anticancer drugs in an array of configuration (Lobatto *et al.,* 2001).

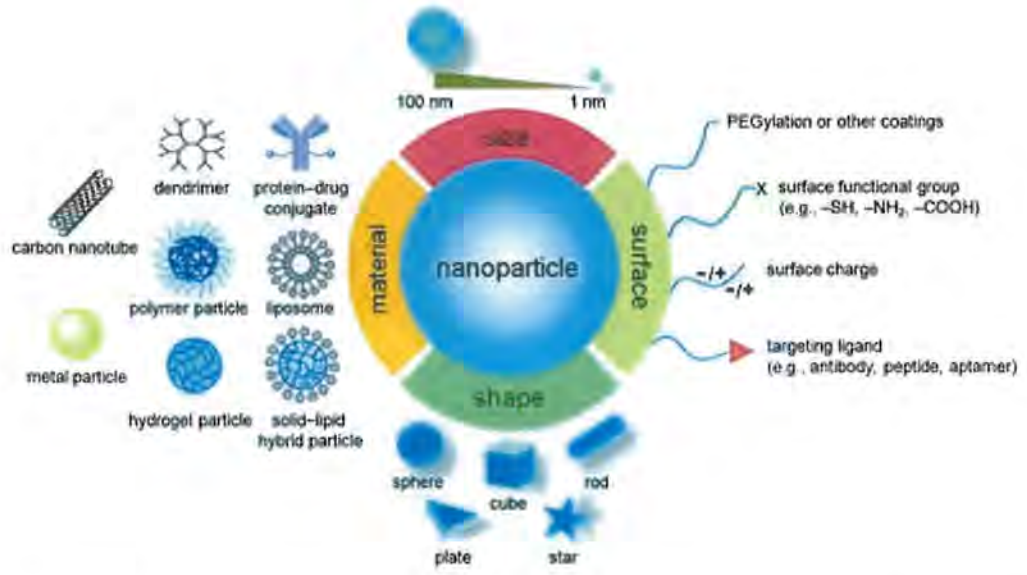

Figure 1.7 Nanoparticles as carriers for drug delivery in cancer therapy (Sun *et al.*, 2014)

1.9. Nanomedicine

Nanotechnology relies on manipulating chemical and physical properties of the matter at the atomic and molecular scales and it has proven to be a quickly developing industry (Fulekar *et al.*, 2014). Making engineered nanoparticles is a main focus that incorporates utilization of different starting materials like metals, non metals, metal oxides, carbon polymers and lipids (Grillo *et al.*, 2015).

1.9.1. Use of Nanomedicine in Therapeutics

To produce nanomedicine by the use of nanotechnology is an emerging field universally, where elements of nanometer size, frequently between 1 to 100nm, are

utilized in creating nanodrugs with biological applications (Sinha *et al.*, 2006). Nano materials can be utilized with a variety of biological macromolecules and proteins (Faraji and Wipf, 2009). The most common applications of nanoparticles consist of diagnosis, treatment and disease control involving quantum dots, nanowires, liposomes, and carbon nanotubes etc. In the field of medicine and physiology, nanomedicine is an emerging trend (Singh *et al.*, 2008). Nanoparticles' properties can be altered by altering their structure, size and surface area. Compared to other particles such as microparticles, they offer high surface to mass ratio (Thomas *et al.*, 2005). Various functional groups can be employed to alter the surface of these nanoparticles. Nanoparticles in therapeutics are used as vehicles for communication of molecular and cellular components because of size similarities with biomolecules (Firaji and Wipf, 2009). The drug can be coupled covalently on the surface of nanoparticles to make a working therapeutic solution (Mohanraj *et al.*, 2006).

1.10. Nanomedicine Targeting

The two major components of drug targeting are target and carrier. Target is acute or chronic group of cells/organs which have to be treated, while carriers are particular molecules attached to a drug which alter their configuration at molecular level and transfer drug to target specific sites.There are four different types of drug targeting so far:

1. Passive Targeting (Haley and Frenkel, 2008).

2. Active Targeting (Danhisher *et al.*, 2010).

3. Stimuli Responsive Drug Delivery (Lammers *et al.*, 2012).

4. Targeted Drug delivery (Wilczewska *et al.*, 2012).

1.11. Types of Nanoparticles

Nanoparticles are of two types: synthetic and naturally occurring. Different types of nanoparticles are produced, characterized and utilized in various therapeutic systems such as polymeric, magnetic, carbon nanotubes and inorganic nanoparticles (Sanvicens and Marco, 2008).

1.11.1. Magnetic Nanoparticles

Magnetic nanoparticles frequently have Fe^{2+} and Fe^{3+} as central metal atom, surrounded by PEG or dextran. Their size ranges from 10 to 20 nm and are spherical

in shape. They have enormous *invitro* and *invivo* applications such as bioassays (Sanvicens and Marco, 2008). They are activated by the magnetic field and are dynamically taken up by desired tissue. They may follow passive or active targeting in case of drug targeting. They could not be used in drug delivery system because of loss of nano-sized feature due to aggregation (Arruebo *et al.*, 2007).

1.11.2. Polymeric Nanoparticles

The size of polymeric nanoparticles ranges from 10 to 1000nm with solid structures. They have gained much importance because they are easily degradable in living systems. They can be utilized in drug delivery specifically as they have the features of controlled drug release and can carry biomolecules (Soppimath *et al.*, 2001). Glycolic acid and lactic acid are released when they are degraded. The degradation of polymeric nanoparticles does not cause any damage such as toxicity, immunogenicity, thrombogenicity or inflammation to living system (Wilczewska *et al.*, 2012).

1.11.3. Inorganic Nanoparticles

Inorganic nanoparticles have ceramic composites like silica or alumina etc. They may be arranged in mesoporous or hollow form and provide large surface area. They could be porous facilitating drug take-up and giving protection to drug from denaturation or degradation (Faraji and Wipf, 2009).

1.12. Characterization of Nanoparticles

For the characterization of nanoparticles, usually following techniques are used:

- Fourier transform infrared spectroscopy
- X-ray diffraction analysis
- Zeta potential
- UV visible spectroscopy
- Scanning electron microscopy

1.12.1. X-ray Diffraction Analysis (XRD)

X-ray powder diffraction (XRD) isa technique, utilized for the quantitative and qualitative analysis of crystalline compound. It identifies material type, size, purity of the sample, orientation and explains the structure of the crystal such as geometry and lattice constants etc (Hassellov *et al.*, 2008). In this process, monochromatic x-ray beam is passed through the sample which results in diffraction of x-rays to precise

angles at diverse positions with specific intensities. Bragg's equation is used to measure inter-particle spacing (Tiwary *et al.*, 2013).

Bragg's equation:$2dsin = n\lambda$

Where, d is the inter-planer spacing, n represent order of reflection and λ represents wavelength of incident radiation.

1.12.2. Ultraviolet Visible Spectroscopy (UV/VIS)

UV/Vis spectroscopy is utilized for the quantitative determination of non metals and metals. It is a basic technique for verification of nanoparticles synthesis by characteristic peaks that arise because of specific Surface Plasmon Resonance of nanoparticles. Different factors such as temperature, pH, dielectric constant and size of nanoparticles influence the absorption peaks (Ramamurthy *et al.*, 2013). It is also helpful for determination of concentration and stability of nanoparticles (Haiss *et al.*, 2007).

1.12.3. Fourier Transform Infrared Spectroscopy (FTIR)

FTIR tells us different types of functional groups involved in the production and stabilization of nanoparticles. Spectra are recorded at mid infrared regions such as 400 to 4000cm^{-1}on spectrophotometer. Development of new entity by drug loading is ensured by FTIR and shows absorption bands of particular functional groups which tell characteristics of protein spectra (Sarmento *et al.*, 2006).

1.12.4. Zeta Potential

Zeta potential can be utilized to derive information concerning the molecule's surface charge.It is the potential generated between the charged groups at the surface of the particle and the suspension medium (Butt *et al.*, 2004).

1.13. Cerium Oxide Nanoparticles

Cerium is placed in the lanthanide series of the periodic table with 4f electrons. It has attracted a lot of attention from researchers in chemistry, physics, biology and material sciences. Ehen combined with oxygen, Cerium Oxide takes on fluorite crystalline structure in a nanoparticle formulation and appears as a fascinating material (Conesa, 1995). Cerium nanoparticles have been employed effectively in a variety of biological and engineering applications for-example catalytic materials, solid oxide fuel cells, solar cells, high temperature oxidation protection materials and

potential pharmacological agents (Kaspar *et al.*, 1999; Patel *et al.*, 2002; Ceraldo *et al.*, 2011). Cerium Oxide nanoparticles can vary reversibly from Ce^{3+} to Ce^{4+} thus creating oxygen vacancies, which show redox potential (Perez *et al.*, 2008; Wang *et al.*, 2013).

CeO_2 nanoparticles have turned out as a fascinating material in genetics field and used in drug delivery, biomedicine, bioanalysis and bioscaffolding (Ceraldo *et al.*, 2011; Lin *et al.*, 2012; Xu *et al.*, 2013). Cerium oxide demonstrates active changing from Ce^{4+} to Ce^{3+} in an acidic environment, though the higher oxidation state increasingly becomes stable in basic environment. On account of its capacity to change between varied oxidation states, Cerium Oxide nanoparticles have excellent antioxidant properties (Jimmy *et al.*, 2003; Micheal and Hochella, 2008).

Cerium Oxide nanoparticles demonstrate a pH dependent impact on ROS production (Alili *et al.*, 2011).Cerium Oxide nanoparticles act as a scavenger of H_2O_2 in neutral tissues; however, in an acidic environment they act as a producer of H_2O_2 (Wason *et al.*, 2013). Numerous factors such as particle size, shape, surface chemistry and surface additives or ligand that can take part in redox reactions have an influence on the pro and anti oxidant properties of the Cerium Oxide nanoparticles (Dowding *et al.*, 2013; Kumae *et al.*, 2014).

1.14. Cerium Oxide Nanoparticles and Cancer

A major cause of changes in cell and hereditary alterations including cancer is reactive oxygen species (ROS). The accumulation of reactive oxygen species in cells is usually related to undesired consequences. ROS production, which also consists of reactive Nitrogen species give rise to neurodegenerative diseases, diabetes, aging and cancer.ROS can generate the expansion and progression through remarkable variation to oxidative pressure and deregulation of antioxidant enzyme configuration in cancer (Waris and Ahsan, 2006). Specifically, Cerium nanoparticles exhibit strong anti oxidant action, averting oxidative stress, damage to the cell and death by apoptosis (Ceraldo *et al.*, 2011; Caputo *et al.*, 2015). Cerium nanoparticles cause a decline in the elevated levels of H_2O_2 (Pirmohamed *et al.*, 2010; Dowding *et al.*, 2013). Figure 1.10 shows the dual properties of Cerium Oxide nanoparticles.

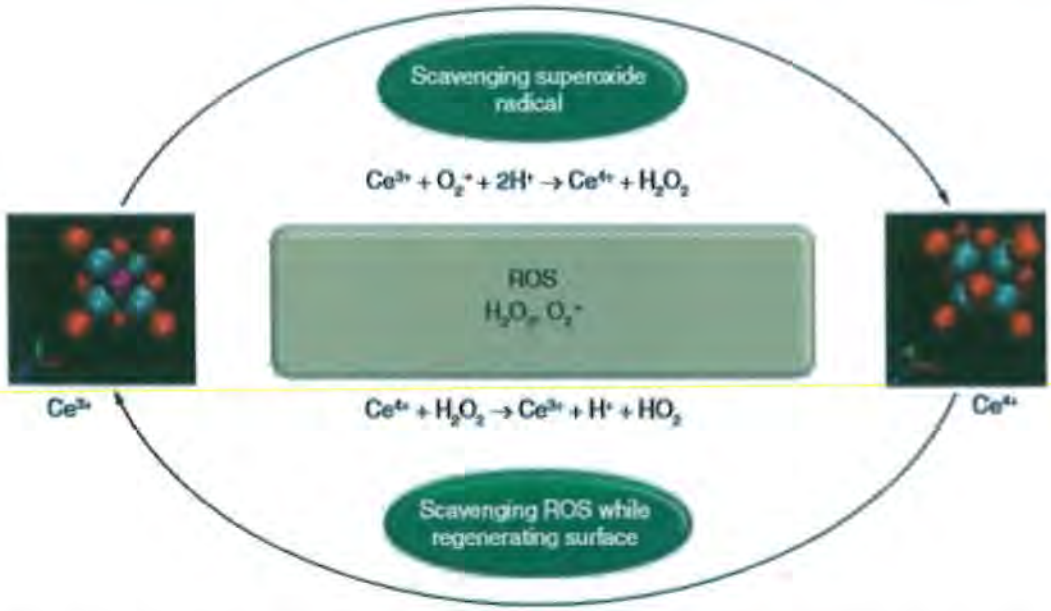

Figure 1.8 Scavenging properties of Cerium Oxide nanoparticles (Das *et al.*, 2013)

1.15. Therapeutic Index

Nano-formulation in medicine is spreading swiftly to increase drug uptake and delivery to specific sites. In this case nanoparticles are utilized because they have the potential to lessen toxicities caused to healthy cells because of increased therapeutic index. Therapeutic index is the comparative analysis of the efficacy of drug on pathological tissues to the cytotoxicity it causes to other normal tissues (De Jong and Borm, 2008).

1.16. Annexin V Binding Assay

Annexin V, a technique to detect apoptotic cells, was first reported by Koopman *et al*, in 1994 (Koopman *et al.*, 1994). Succeeding studies showed that Annexin V staining procedure could be utilized to identify apoptotic cells, in various settings regardless of the stimulus used to activate apoptosis or the heredity of the cells under examination (Martin *et al.*, 1994; Fadok *et al.*, 1998).Annexin V, belongs to phospholipid-binding Annexin family. It binds in a reversible and Ca^{2+} dependent manner to phosphotidylserine and to a lesser extent to sphingomyelin and phosphotidylcholine (Gerke, 2001; Gerke, 2002).

Numerous studies have demonstrated that phosphatidylserine (PS), a phospholipid usually maintained in the inner leaflet of the plasma film, plays an important role for

phagocytes in the recognition of the apoptotic cells. Ordinarily, PS is effectively sequestered in the inner layer of plasma membrane through the activity of calcium dependent scramblase and an amino phospholipid translocase (Fadok *et al.,* 1998). PS is transported from the internal to external surface of the plasma membrane, upon receiving pro apoptotic signals and it acts as early signal of the apoptosis (Fadok *et al.*, 1992; Martin *et al.,* 1995).

1.17. qPCR Relative Expression Analysis

To determine the effectiveness of a drug on genetic basis the qPCR is usually performed. Before and after the drug administration changes in target gene expression can be identified. We selected some of the target genes to determine that whether or not Cerium Oxide nanoparticles show apoptotic effects at genetic level in leukemic rats.

1.17.1. NF-kappa B Pathway

NF-kappa B is a transcription factor and it exhibits a major role in a wide variety of physiological processes. NF-kappa B plays a central function in the homeostasis, development and stimulation of the immune system and it is also regulator of the epithelial homeostasis (Ghosh and Hayden, 2012). NF-kappa B is a group of interrelated transcription factors, Rel A/p65, Rel B, c-Rel, p50 and p52 and by homo or hetero dimerisation they form 12 distinctive identified dimers. A conserved Rel homology domain that encourages dimerisation and DNA binding is contained by all NF-kappa B subunits. The Rel A, Rel B and c-Rel subunits also have a transactivation domain which carries the transcriptional activity of dimers including these subunits (Hoffmann *et al.,* 2006). Several cancer cell types contain elevated levels of NF-kappa B transcription factors such as Rel A, c-Rel and Rel B (Karin *et al.,* 2002). Numerous kinds of tumor cells have been reported to show constitutively active NF-kappa B such as leukemia, lymphoma, melanoma, colon, breast, prostate, myeloma, pancreas, head and neck and squamous cell carcinoma cell lines (Mor *et al.,* 1999; Mukhopadhyay *et al.* ,2001).

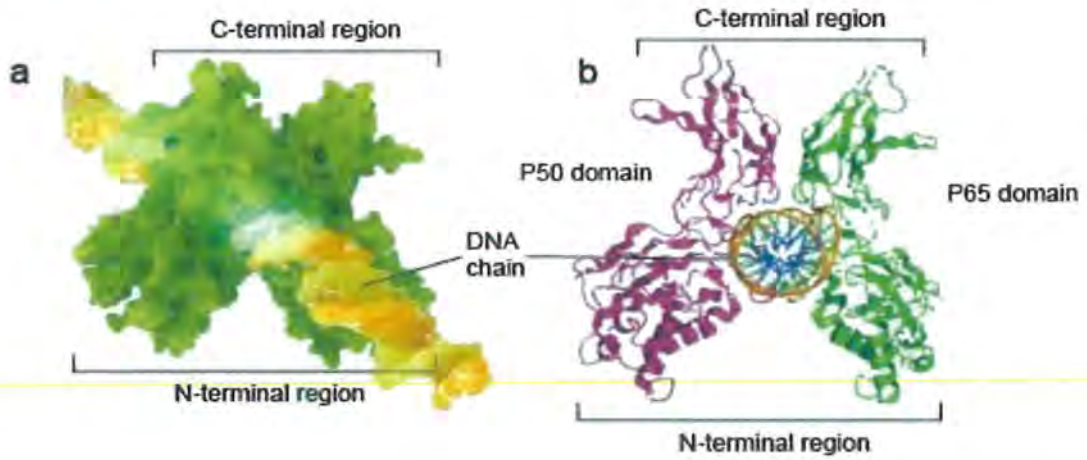

Figure 1.9. Structure of the NF-kappa B protein dimers binding with DNA chain (Oeckinghous and Ghosh, 2009).

1.17.2 TRAIL Pathway

The major anti-cancer treatment approach in tumor cells is to induce apoptosis (Johnstone *et al.*, 2002). Two of the major molecular signaling pathways that are responsible for apoptotic cell death are intrinsic pathway and extrinsic pathway. The intrinsic pathway is stimulated by the signals from the members of the B- cell leukemia/lymphoma within the cell and from downstream mitochondrial signals. The extrinsic pathway is stimulated by proapoptotic ligands from outer surface of the cell and act together with particular cell surface death receptors (Ashkenazi, 2002). TRAIL is a part of the TNF-superfamily of ligands and it is a type II transmembrane protein (Lawrence *et al.*, 2001). Crosstalk between the extrinsic and intrinsic apoptotic signaling pathways take place at several points forming a complex and intricately balanced system (Spencer and Sorger,2011).

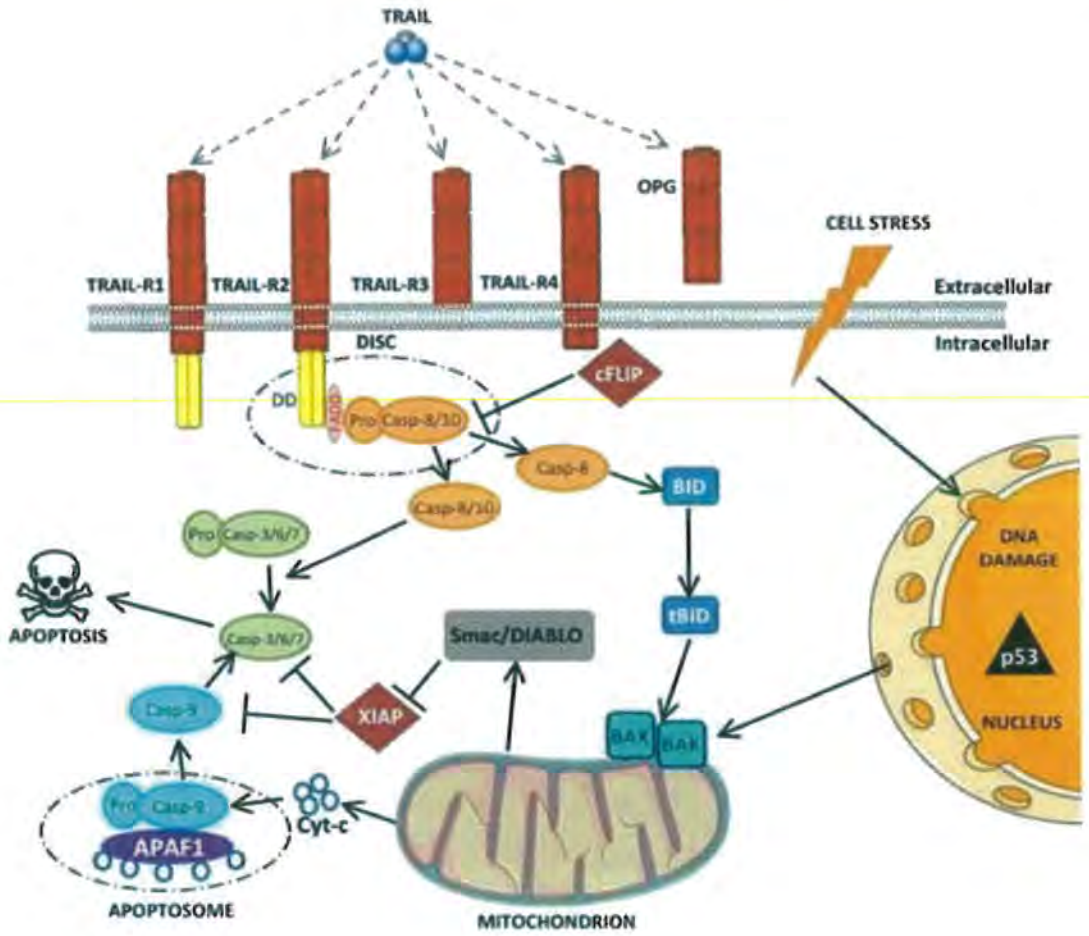

Figure 1.10 TRAIL pathway and apoptosis overview (Stuckey and Shah, 2013)

1.18. Aims and Objective

The purpose of the study was to find out the efficacy of cerium oxide nanoparticles against leukemia and to check the effects of the complex of cerium oxide nanoparticles and doxorubicin in the form of nanomedicine. The main objectives of this study were as follows:

- To synthesize and characterize Cerium Oxide nanoparticles and develop encapsulated drug.
- To induce leukemia in rats by benzene injections and study the effects of nanomedicine on blood parameters of leukemic rats.
- To measure rate of apoptosis in leukemic and treated rats.
- To measure hepatic enzymes activities in leukemic and treated rats.
- To measure anti-oxidant enzymes activities in leukemic and treated rats.
- To determine changes in relative gene expression of proliferative and tumor suppressor genes after nanomedicine administration.

2. Materials and Methods

All molecular assays in-vitro and in-vivo were carried out under standard conditions, with optimized protocols. Institutional Review Board (IRB), of Quaid-i-Azam University, Islamabad approved this study.

2.1. Cerium Oxide (CeO_2)Nanoparticles Synthesis

Materials

Cerium chloride ($CeCl_3$), Ammonium Hydroxide (NH_4OH)(from Sigma Aldrich).

Procedure

Cerium oxide nanoparticles can be synthesized by different ways. But here we used chemical method for the synthesis of cerium oxide nanoparticles. By means of a simple chemical precipitation technique CeO_2 nanoparticles were produced. 3.7 grams of Cerium chloride ($CeCl_3$) were dissolved in 100ml distilled water and stirred moderately at 70°C. When the temperate reached to 70°C, 50 ml of Ammonium hydroxide solution (10%) was poured drop wise into the solution. After complete addition, the mixture was further stirred at the same temperature for almost 5 hours. The solution was then allowed to cool until room temperature was attained. The solution was then centrifuged for 10 minutes at 10,000 rpm. The precipitate obtained was further washed five times by distilled water via centrifugation followed by oven drying at 80°C. The dried, pale yellow precipitate was carefully ground in mortar and pestle to obtain fine powder. Finally, the obtained powder was calcinated at 400°C for 2 hours.

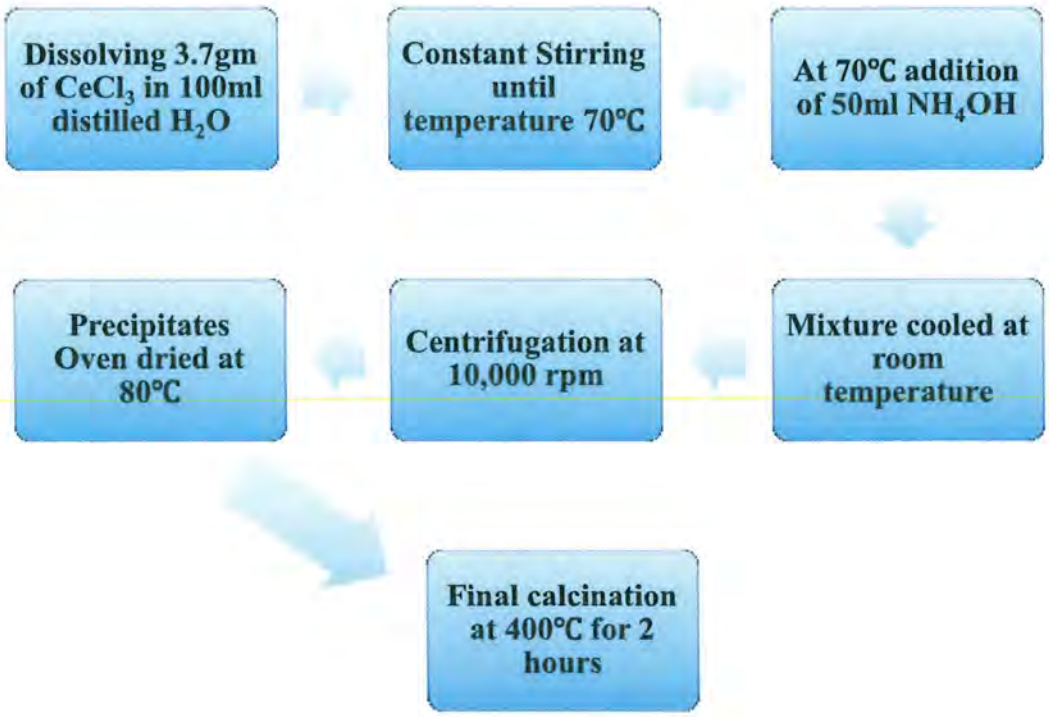

Figure 2.1 Steps involved in the synthesis of Cerium Oxide Nanoparticles

2.2 Characterization of Nanoparticles

The yellowish powder obtained after calcinations was then examined to confirm the synthesis of Cerium Oxide nanoparticles. For this purpose, cerium oxide nanoparticles were characterized by XRD (Bucker D8 Advance, Germany), UV/VIS spectroscopy (Perklin Elmer UV/Vis- Lambda 25), FTIR, Zeta potential (Malvem Instruments Worcestershire, UK).

2.2.1. X-ray Diffraction Spectroscopy

XRD analysis of synthesized CeO_2 nanoparticles was performed on X-ray spectrophotometer (Bucker D8 Advance) equipped with Cu-Kα radiation (α=1.54nm) in the 2θ range 10°-80°. To obtain the average crystalline size Scherrer equation was used using the most intense peak of the diffractogram using the following equation

$K\alpha/B \cos \theta$

Here k is a dimensionless form factor,τ denotes mean crystallite size, λ is describing wavelength of the coming X-rays and β is the width at the mean peak height and finally θ which shows the diffraction angle.

2.2.2. Size Distribution and Zeta Potential

Size distribution and Zeta Potential of the prepared samples was obtained by using a Zetasizer Nano-ZS (Malven Instruments, Worcestershire, UK). To measure the approximate size of Ce-nanoparticles and of doxorubicin-Ce nanoparticles complex and to determine the surface charge property, in ultra-pure water a tenfold dilution of the samples were prepared and 1mL of the prepared solution at 25°C was subjected to a particle size analyzer. The calculation was based on the property of particles of electrophoretic mobility which was changed to zeta potential by using inbuilt software based on the Helmholtz-Smoluchowski equation (Morais *et al.*, 2013).

2.2.3. UV/Vis Spectroscopy

UV/Vis spectrophotometer (Perklin Elmer UV/Vis- Lambda 25) was used to get optical absorption spectrum of cerium nanoparticles alone, drug alone and drug loaded nanoparticles in Biochemistry Department, Quaid-i-Azam University, Islamabad. Absorption spectra were recorded in the range of 250-800nm at 25°C.

2.2.4. Fourier Transform Infrared Spectroscopy (FTIR)

FTIR analysis was carried out to determine the functional groups of the nanoparticles and nanomedicine. Liquefied sample (400) was loaded in FTIR spectroscope (Bruker, Tensor 27) with a scanning range of 400 to 4000 cm^{-1} and a resolving power of 4 cm^{-1}.

2.3. Synthesis of Nanomedicine

Nanomedicine was synthesized by doxorubicin coating upon Cerium Oxide nanoparticles for increase biocompatibility and bioavailability.

2.3.1. Drug Loading on Nanoparticles

After synthesizing Cerium Oxide nanoparticles by chemical method, powdered doxorubicin was loaded on them. This was done by first adding 80 mg of Cerium Oxide nanoparticles in 9 ml of injection water. The solution was set on sonication for 4hours to obtain a miscible solution. After this, 18.7mg of doxorubicin was added to the nanoparticles and were kept on overnight stirring to obtain nanomedicine.

2.3.2. Loading Efficiency of Drug

Some of the doxorubicin used for loading on nanoparticles remains unattached, so it is necessary to find the amount of unloaded drug. Percentage of drug loading and entrapment was calculated according to procedure followed by Jiao *et al.*, 2012 with minor modifications. 1ml of prepared nanomedicine was centrifuged at 5000g for 20minutes. UV/Vis spectrum at 200nm length is noted.

$$\text{Drug loading} = W1/W2 \times 100$$

$$\text{Encapsulation Efficiency} = W2- W3/ W2 \times 100$$

Where W1 is the weight of the doxorubicin in nanomedicine, W2 is the nanomedicine and W3 is the amount of drug that remained in supernatant.

2.4. Brine Shrimp Assay (Cytotoxicity Assay)

By using brine shrimp eggs, we performed an assay to determine the optimum dosage of drug and nanomedicine (requirements are given in table 2.1).

Table 2.1: Requirements for Brine Shrimp Assay

No.	Materials	Quantity	Company name
1.	Brine shrimp eggs	As required	Ocean star international, Inc
2.	Sea salt	17g	-
3.	Distilled water	500mL	-

Brine shrimp eggs were added to the sea salt and allowed to incubate under fluorescent light and hatch at 37^0Cfor 24 to 36hours in sea salt solution. 17g of sea salt was added in 500mL of distilled water to prepare sea salt solution. Following dilutions were prepared in triplets to determine cytotoxicity at various concentrations.

Table 2.2 Dosage Regime for Brine Shrimp Assay

Drug	Conc. 1	Conc. 2	Conc. 3	Conc. 4
CeO_2 Nps	5mg/	2.5mg/	1.25mg/	0.625
Doxo	4.2mg/	2.1mg/	1.05	0.525
CeO_2+Doxo	2.5mg/ 500ul + 2.1mg/ 500ul	1.25mg/ 500ul + 1.05mg/ 500ul	0.625mg/ 500ul + 0.525mg/ 500ul	0.3125mg/ 500ul + 0.625mg/500 ul

The serial dilutions were prepared in 96 well microplate and dried overnight at room temperature. Next day, 10 brine shrimp eggs were counted with the help of magnifying glass and placed in each well for 24 hours. The number of alive and deadeggs were calculated under the microscope to calculate the lethal concentration (LC 50 value) of dilutions.

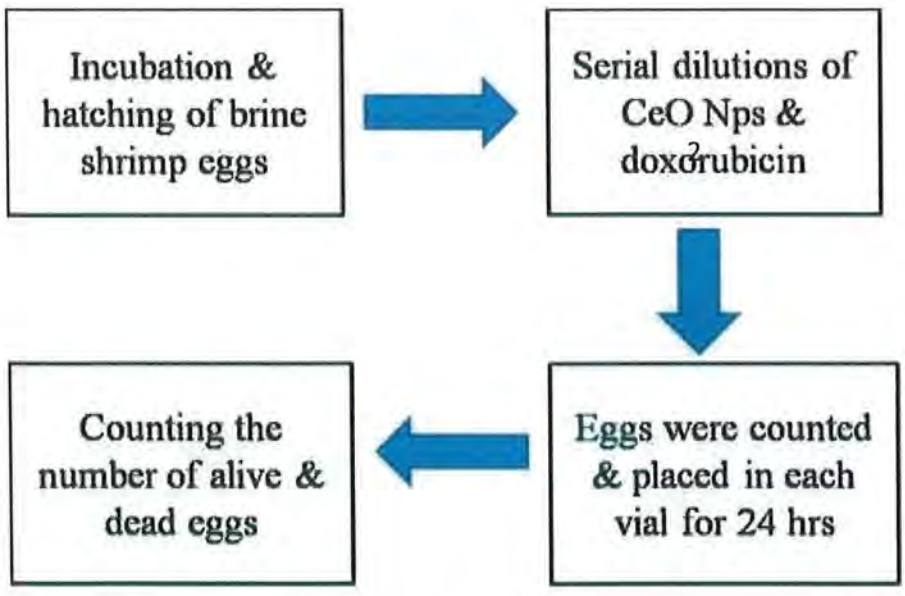

Fig. 2.2 Steps involved in Brine Shrimp Assay

Figure 2.3 Visual representation of Brine Shrimp Assay

2.5. Experimental Strategy

For *in vivo* studies, National Institute of Health (NIH), Islamabad was approached for purchasing 15 Sprague Dawley rats, which were then kept under standard conditions in Primate Facility, Quaid-i-Azam University. The 15 rats were then classified into five different groups, each group having 3 rats and labeled correspondingly. The rats were handled according to guidelines directed by Ethical Committee of Quaid-i-Azam University (BEC-FBS—QAU-09).

Table 2.3 Mode of Administration of drugs

Groups	No of Rats	Dosing	Mode of Administration
1. Normal	3	Normal saline	Intraperitoneal
2. Leukemic	3	0.2 mL benzene alternatively for 3 weeks	Intraperitoneal
3. CeO_2 Nps	3	0.3 mL alternatively for 3 weeks after benzene treatment	Intraperitoneal
4. Doxo	3	0.3 mL alternatively for 3 weeks after benzene treatment	Intraperitoneal
5. CeO_2 Nps + Doxo	3	0.3mL alternatively for 3 weeks after benzene treatment	Intraperitoneal

2.5.2. Administration of Benzene

Benzene dosage were prepared by using injection water, benzene and isopropanol in the ratio (1.5:2:1.5) and 0.6ml of injection water was mixed with 0.8ml of benzene and 0.6ml of isopropanol. 0.2ml of the dose was injected intraperitoneally to each rat of groups 2, 3, 4 and 5. The injections were given at alternate days for three consecutive weeks under optimized and standard conditions. Group 1 was given normal saline and was considered as negative control.

2.5.3. Cerium Nanoparticles

After confirmation of leukemia by hematological studies, group 3 was given chemically synthesized cerium nanoparticles. Stock solution of cerium nanoparticles was prepared by mixing 48.6 mg of CeO_2 in 5400µl of injection water. The cerium nanoparticles were sonicated for 15 minutes before *invivo* administration.CeO_2 were injected intraperitoneally twice weekly for 3 weeks.

2.6. Animal Dissections

All rats were dissected after completion of doses, according to rules of Institutional Animal Care and Use committee (IACUC). Chloroform was used to anesthetize the rats and surgical tools were used to cut the abdominal cavity to collect various organs such as heart, liver and kidneys for further processing. All

the organs were weighed by the help of weighing balance and the recorded data were used for measuring relative organ weight. The organs were stored at -80°C for relative expression studies.

2.6.1. Blood Collection and Storage

The blood was taken directly from the heart by using heparinized syringes and placed in commercially available Ethylene Diamine Tetra Acetate (EDTA) tubes and serum tubes immediately. EDTA tubes were stored at -4^0C. To separate the serum, serum tubes were centrifuged at 3000rpm for 15minutes and stored at -40^0C to prevent hemolysis.

2.7. Blood Profiling

Blood smears were prepared on glass slides by using fresh blood for morphological analysis. Blood drop was placed 1-3cm from top and then sliding cover slip upon blood dot at 45° angle; first sliding backward and then forward till the end of the slide. The smears were then air dried. For fixation of the cells, the slides were dipped in chilled absolute methanol for 10 minutes. The slides were again air dried and then Giemsa dye was poured drop wise on the slides and left for 10 minutes. The stained slides after washing with tap water were air dried. To study the morphology of the cells the slides were observed under the light microscope at 100X.

2.8. Complete Blood Picture

Blood CP was calculated to obtain total blood cell count by using automated blood analyzer that determines a variety of blood parameters. For this reason, 100µl of blood was stored in EDTA tubes and transferred to Islamabad Diagnostic Centre for Blood CP. The complete blood picture comprised of WBC, RBC, PLT, HGA and other blood parameters.

2.9. Flow Cytometry

First of all cells were washed twice with cold BioLegends Cell Staining Buffer. After that Annexin V Binding Buffer was used to resuspend the cells at a concentration of 0.25-1 $\times 10^7$ cells/ml. In a 5ml test tube, we transferred 100µl of cell suspension.5µl of FITC Annexin V was added to it. Then 10µl of propidium iodide solution was added to it. The cells were vortexed gently and then at 25^0C,they were incubated for 15minutes in dark conditions. Then in each tube

400µl of Annexin V Binding Buffer was added and analyzed on the flow cytometer.

2.10. Enzymes Activity (Hepatic and Renal)

Micro Lab 300 auto analyzer (Merk) was utilized to execute biochemical assays for the evaluation of enzymes activity. The parameters examined were Alanine Aminotransferase (ALT), Alkaline Phosphatase (ALP), Aspartate aminotransferase (AST) and Renal Function Test by using biochemical analysis kits (AMP diagnostic kits).

2.10.1 Alkaline Phosphatase (ALP)

Standard protocols provided by AMP diagnostic kits were used to estimate the quantity of Alkaline Phosphatase. About 1mL of Reagent A was added in an Eppendorf tube following the addition of 20µL of serum. At 37°C the solution was incubated for 1 minute, then 250µL of Reagent B was added to the solution. Absorbance was taken with the help of Micro Lab 300 auto analyzer (Merk) at 420nm for 1 minute. Reagents mixture without sample was taken as blank. 3 readings were taken consecutively.

A/min × 2757= ALP activity U/L

2.10.2 Alanine Aminotransferase (ALT)

LTA diagnostic kit was used to perform ALT assay. We utilized 1000µl of Reagent 1 (Tris buffer 100mM at pH 7.15, preservatives and stabilizers) and 250µl of Reagent 2 (L-alanine 500mM, alpha-keto glutarate 12mM, NADH 0.18mM, LDH > 1700 U/I) in an eppendorf. In Reagent 1, 125µl of serum sample was mixed by vortexing and left for 5minutes at room temperature. After adding Reagent 2, the mixture was added to the auto analyzer by its sipper and initial absorbance reading was recorded. To determine difference between absorbance values three readings were taken after every 1 minute.

A/min × 1746= ALT/GPT activity U/L

2.10.3 Aspartate Transferase (AST)

Working reagent was prepared according to instructions given by LTA diagnostic kit to assess the enzymatic action of AST. At 340nm, spectrophotometer was zeroed with distilled water. 1 mL working reagent was added to the cuvette, to the control and to each sample, and for 3 minutes heated at 37^0C. Then 100uL

serum was added to each tube and mixed gently. By means of spectrophotometer, absorbance was recorded at 1 minute. The sample was incubated at 37^0C and again absorbance was taken at 2 and 3 minutes. The average absorbance per minute was multiplied with factor 1746 for results in U/L.

U/L = A/Min × 1746

2.11. Relative Expression Analysis

2.11.1. Total RNA Extraction

Quantitative Real Time PCR was performed to study the relative expression at RNA level. RNA was extracted by the TRIZOL method. The liquid nitrogen preserved tissues were utilized to extract RNA by the use of optimized extraction protocols. 100mg frozen tissue was weighed and added in 1ml TRIZOL and the tissue was homogenized by means of electric homogenizer. As a result of homogenization a dust like liquid was observed, and was shifted to an eppendorf. 200µl chilled chloroform was added to it after incubation for 5minutes at room temperature. The mixture was shaken vigorously to obtain baby pink color. The eppendorf was centrifuged at 12000rpm for 15 minutes at 4^0C after incubation for 2 minutes at room temperature. After centrifugation, 200µl of the supernatant was transferred to new chilled eppendorf and pellet was discarded. 200µl chilled isopropanol was added to it. After shaking the solution the eppendorf was incubated on ice for 10 minutes. After incubation on ice the solution was centrifuged at 12000rpm for 10 minutes at 4^0C. Then the supernatant was discarded and 1ml 75% chilled ethanol was added to it to wash the pellet. Then it was centrifuged at 7,500 rpm for 5minutes at 4^0C. Supernatant was discarded and pellet was washed once again with 75% ethanol. After drying the pellet for 15minutes at room temperature the pellet was then dissolved in 20µl of RNase free water. The extracted RNA was then quantified by Nano Drop and it was run on 1% Agarose gel for quality assurance. The RNA from liver was extracted by using the above protocol.

Table 2.4 Reagents required for RNA extraction

No.	Chemical Name	Quantity
1.	TRIZOL	1ml/sample
2.	Isopropanol	200µl/sample
3.	Chloroform	200µl/sample
4.	75% Ethanol	2ml/sample
5.	RNase Free Water	20µl

2.11.2. cDNA Synthesis

The extracted RNA from the above process was then processed for cDNA synthesis by using VIVANTIS kit (cDSK01-050). For this purpose, all extracted RNA concentrations were leveled at 3000ng or 3µg. RNA purification was carried out in an RNase-free environment. Two mixtures were prepared i.e. RNA primer mixture and cDNA synthesis mixture to synthesize cDNA from the extracted RNA. RNA primer mixture was prepared by mixing calculated amount of RNA, 1µl of random hexamer and 1µl of 10mM dNTPs and keeping the total volume up to 10µl by adding nuclease free water. The mixture was then incubated at 65^0Cfor 5 minutes and then chilled on ice for 2 minutes. The mixture was then spun down for short time.

Table 2.5 Reagents for RNA Synthesis Mixture

S.No	Component Name	Amount/Volume
1	Template- Total RNA	1-10µg
2	Random hexamers	1µl
3	10mM dNTPs mix	1
4	Nuclease-free water	Top up to 10µl

cDNA synthesis mixture was prepared by taking 2µl of 10X Buffer M-MuLV, 0.5µl reverse transcriptase, and nuclease free water upto a final volume of 10µl. 10µl of

the cDNA synthesis mixture was added to each RNA primer mixture. The mixture was briefly spun and after centrifugation, it was incubated for 60 minutes at 42^0C. The reaction was completed by incubating the tubes for 5minutes at 85^0C. The tubes were chilled on ice and centrifuged briefly. Synthesized cDNA was stored at -20^OCuntil further use.

Table 2.6 Reagents for cDNA Synthesis Mixture

S.No	Chemical Name	Amount/Volume
1.	10X Buffer M-MuLV	2µl
2.	M-MuLV Reverse Transcriptase	0.5µl
3.	Nuclease-free water	Top up to 10µl

2.11.3. PCR Amplification

Conventional PCR was performed to confirm cDNA synthesis. This was carried out to assess the annealing temperature of designed primers along with cDNA confirmation. By using integrated DNA Technologies tool, primers were designed. The reagents used in the 25ul reaction mixture are enlisted in table 2.8.

Table 2.7 Reagents for PCR

No	Reagents	Quantity
1.	10X Taq Buffer with $(NH_4)_2SO_4$	2.5µl
2.	$MgCl_2$ 25mM	1.5µl
3.	dNTPs (10mM)	0.5µl
4.	Taq DNA polymerase	0.2µl
5.	Forward Primer	1µl
6.	Reverse Primer	1µl
7.	cDNA sample	1µl
8	DNase free distilled water	17.3µl
	Total Reaction Volume	25µl

After brief vortexing of tubes, they were spun at 8000rpm for 30 seconds after the preparation of reaction mixture. The tubes were then positioned in Thermocycler (Biometra, Germany) and the reaction conditions for the amplification reaction were set as follows.

Table 2.8 Steps involved in Conventional Polymerase Chain reaction

S.No	Steps	Temperature	Duration	Cycles
1.	Initial denaturation	95°C	10 minutes	
2.	Denaturation	95°C	1 minute	40 cycles
3.	Annealing	60°C	1 minute	
4.	Extension	72°C	45 seconds	
5.	Final extension	72°C	10 minutes	
6.	Hold	4°C		

The amplified product after the PCR completion was run on 2%Agarose gel. A standard marker was also run in order to confirm the size of the amplified PCR product.

2.11.4. Agarose Gel Electrophoresis

Agarose gel electrophoresis was carried outto visualize PCR products. The PCR product was run on 2%Agarose gel. The gel was prepared by addition of 1gm of powered Agarose in 50ml of 1X TBE buffer. The Agarose was added to the TBE buffer in a conical flask and was heated in a microwave oven for 2-3 minutes. When the Agarose melted completely, then 6ul of 1% Ethidium bromide was added as a tracking dye. The comb was placed in gel as it was allowed to cool and solidify for 20 minutes. The comb was removed without distorting the wells after solidification. The gel tank (Biometra, Germany) was filled with 1X TBE running buffer and gel was moved to the gel tank. The PCR products werespun briefly and 4µl samples were then loaded with 3µl of Bromophenol blue dye. The voltage was set as 110 V, the Ampere was 120 and gel was run for 45 to 50 minutes. The bands were visualized in Gel Doc and results were recorded using Gene-Snap Software.

2.11.5. Primer Designing

Integrated DNA Technologies were used to design PCR primers for qPCR. The NM numbers of candidate genes from gene data base (NCBI) were selected. By using IDT (https://eu.idtdna.com/scitools/Aplication/RealTimePCR/) tool primers were designed. In-Silico PCR (https://genome.ucsc.edu/cgi-bin/hgPCR) tool was used to check the specificity of the primers. Primers giving specific product and single hit were selected for purchase and further processing. The lyophilized primers were suspended in ultrapure nuclease free water.

2.12. Quantitative Real Time PCR

For quantification of amplified cDNA and relative expression analysis, MIC qPCR by Bio Molecular Sciences was used. The steps involved in the quantitative Real Time PCR were as follows.

2.12.2. Reagents for Real Time PCR

The reagents that were used in the real time polymerase chain reaction were:

1. cDNA for each of the sample
2. Forward and reverse primers for each gene
3. Eva green master mixture
4. Nuclease free water

Table 2.9 Reagents required for Real Time PCR

Sr. No	Reagents	Quantity
1	cDNA	5µl
2	Forward Primer	1µl
3	Reverse Primer	1µl
4	Eva green Master mix	1µl
5	Nuclease free water	2µl
	Total Reaction volume	10µl

2.13. Data Analysis

2.13.1. PFAFL Method (Rest tool)

We utilized PFAFL method to analyze the fold changes in gene expression of the samples. Relative Expression Software tool- 384 = Rest- 384- version 2 was utilized

which is a relative real time PCR expression calculation software. Following formula was used in pair wise fixed reallocation Randomization test.

$$R = \frac{(E_{target})^{\Delta CPtarget\ (MEAN\ control - MEAN\ sample)}}{(E_{ref})^{\Delta CP\ ref\ (MEAN\ control - MEAN\ sample)}}$$

2.13.2. Statistical Analysis

The consequences of different treatments given to rats were evaluated in case of in vivo studies. By using graph pad prism software descriptive statistics were figured out. Results were described as mean + standard deviation (SD). Comparison between treatment groups was undertaken by using ANOVA with Duncan's post hoc test to further separate the means. P values <0.05 was later taken as statistically significant.

3. RESULTS

3.1 Analysis of Cerium Oxide Nanoparticles

Various techniques such as XRD, UV-VIS spectroscopy and zeta potential were done for the analysis of the synthesized cerium oxide nanoparticles to confirm the synthesis and loading of the nanoparticles.

3.2 X-Ray Diffraction Analysis

The powdered X-ray diffraction analysis was carried out on the X-ray spectrophotometer (Bucker D8 Advance) to find out shape and size of the cerium oxide nanoparticles. Debye scherrer formula was used to find the average crystalline size.

$$\text{Crystalline Size } Dp = K\alpha/B \cos\theta$$

Dp represents the average crystalline size of the nanoparticles, whereas k is a Scherrer constant which varies from 0.68 to 2.08 k= 0.94 for spherical crystallites with cubic symmetry, X ray wavelength for Mini Xrd Cu kα average = 1.54178Å, B-FWHM of XRD peak is the full width at half maximum, θ is the XRD peak position at one half of 2.

The crystallite size of the nanoparticles (dp)obtained from the calculations was 14.7 nm.

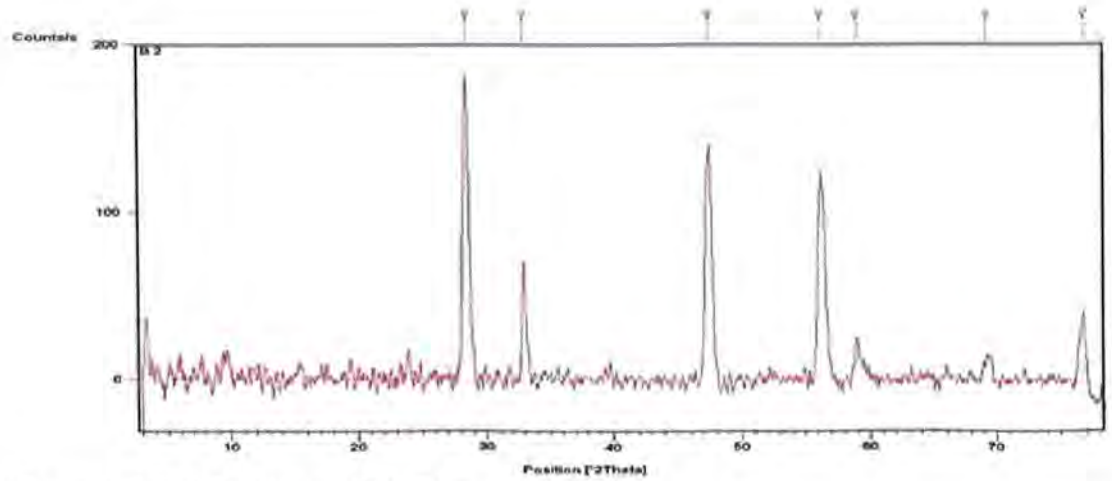

Figure 3.1 XRD Pattern of CeO_2

3.2 Zeta Potential

Zeta potential was done to calculate the charge on the nanoparticles at 25°C. The zeta potential showed that nanoparticles had slightly negative charge on them.

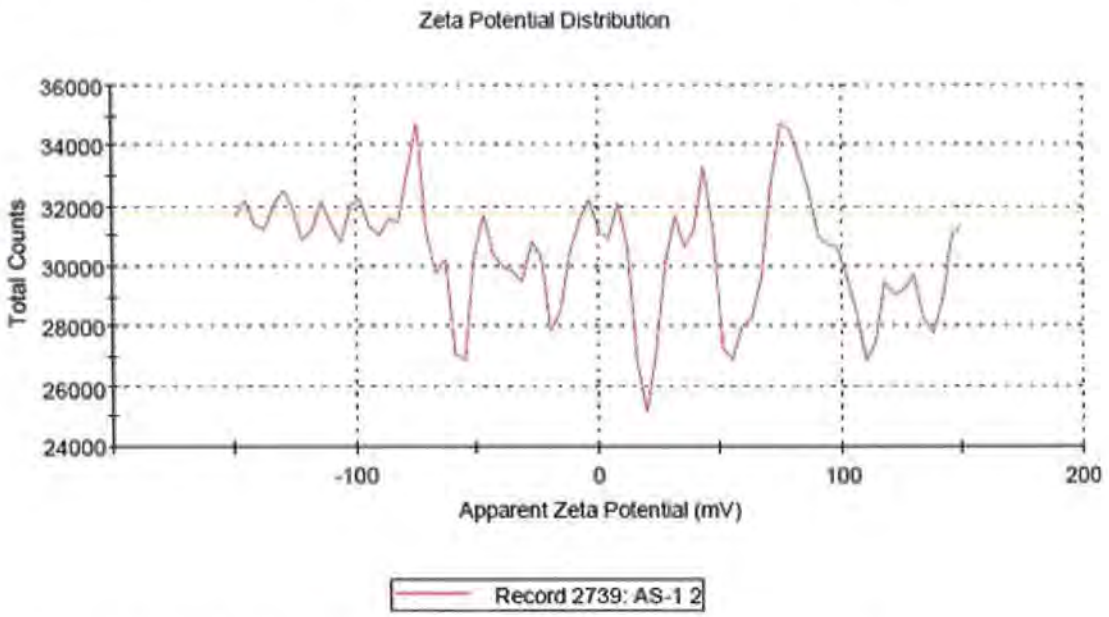

Figure 3.2 shows the zeta potential distribution of nanoparticles

3.3 Loading of the Drug on Nanoparticles

The drug was loaded on the nanoparticles by simple electrostatic interaction. The color of doxorubicin was changed from red to pink through the loading process which indicates that the doxorubicin have formed complexes with Cerium oxide nanoparticles. Panel (A) of figure 3.1.3 represents doxorubicin solution, (B) represents Cerium Oxide nanoparticles solution and (C) represents the nanomedicine. After loading the color of the drug was changed from red and white to pink.

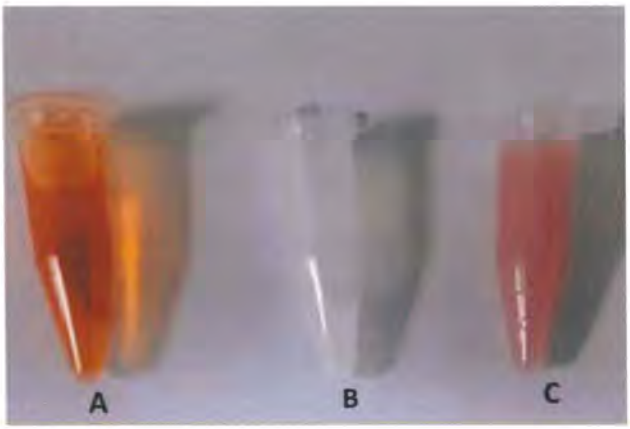

Figure 3.3 Loading of doxorubicin on CeO_2 nanoparticles

3.4 Fourier Transform Infrared (FTIR) Spectroscopy

Absorbance spectra of (a) CeO_2 (b) doxorubicin and (c) nanomedicine was found out by using FTIR spectroscopy. It showed characteristic peaks in the range of 515-3500 cm^{-1}. The peaks in the range of 515-690 cm^{-1} exhibited alkyl halide functional group, 675-900cm^{-1} showed aromatic groups and 1000-1320cm^{-1} represented alcohols, carboxylic acids and ethers.

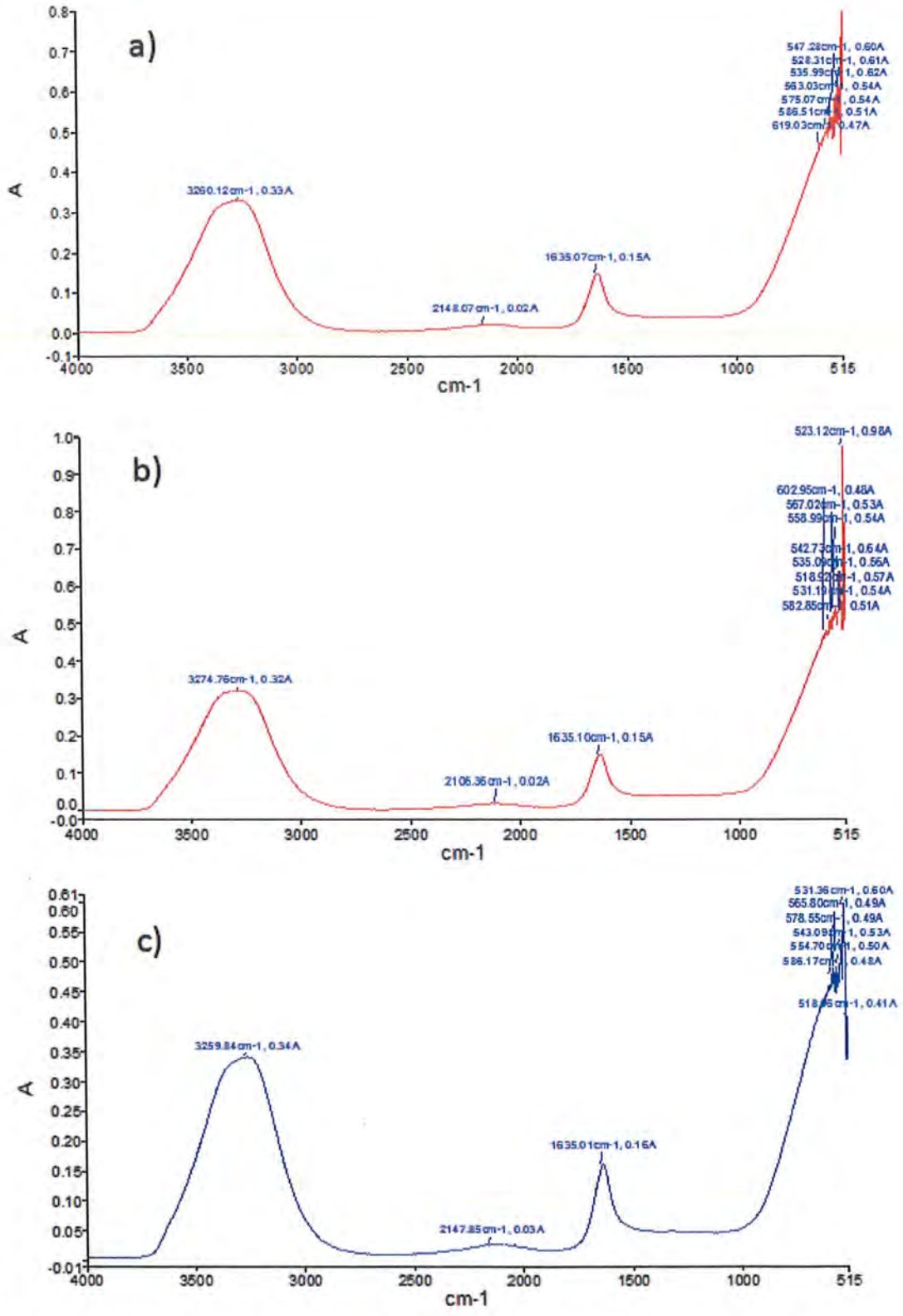

Figure 3.4 FTIR analysis of a (a) CeO_2 (b) doxorubicin (c) Nanomedicine

3.5 UV-VIS Spectroscopy

Optical absorbance was taken in the range of 250 to 800nm. UV-Vis spectroscopy of the CeO_2, doxorubicin and nanomedicine is shown in figure 3.1.5

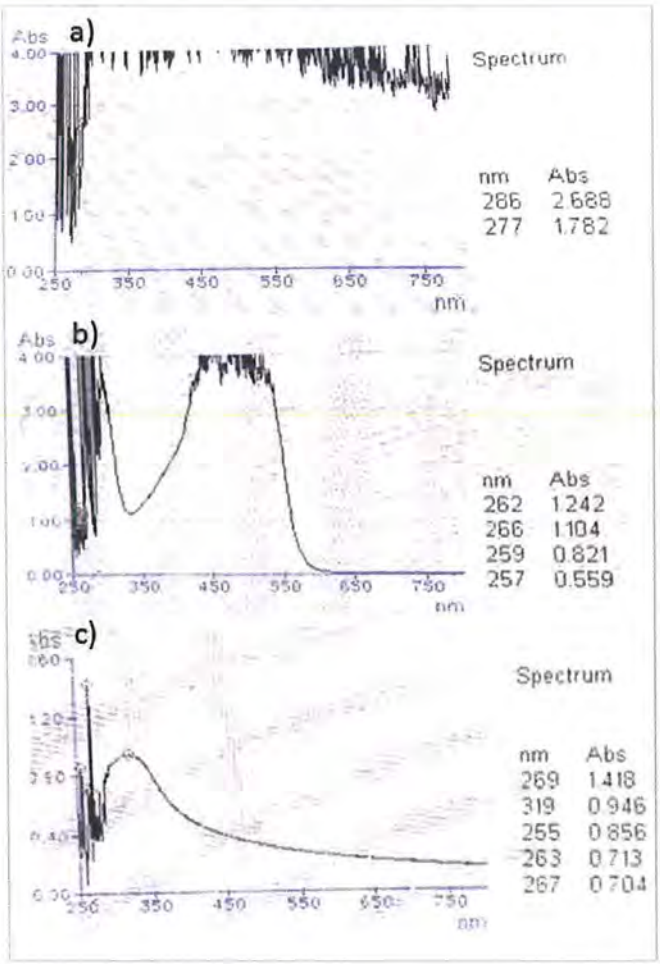

Figure 3.5 Absorbance spectra of (a) CeO_2 (b) Doxorubicin (c) Nanomedicine

3.6 Cytotoxicity Assay

Brine shrimps were utilized for the cytotoxicity assay. Various dilutions of CeO_2 nanoparticles, doxorubicin and combined treatments were checked. Table 3.2 shows the toxicity and lethal concentrations of these compounds. The value of LC_{50} is inversely proportional to the toxicity of compound. (Non toxic> 1000µg/ml, Weak toxic ≥ 500µg/ml, toxic < 500µg/ml).

Table3.1Lethal conc

No	Compo	
1.	Cer	
2.		
3.		

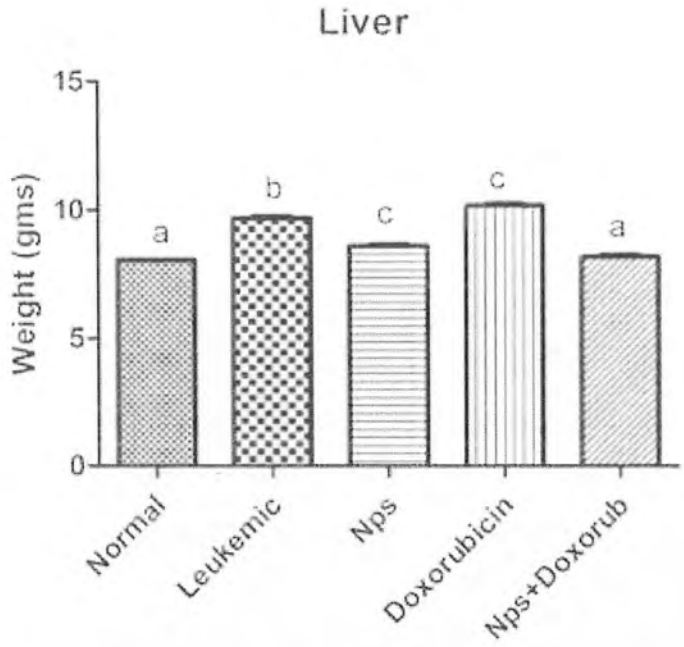

Figure 3.7 Relative liver organ weights in different experimental groups

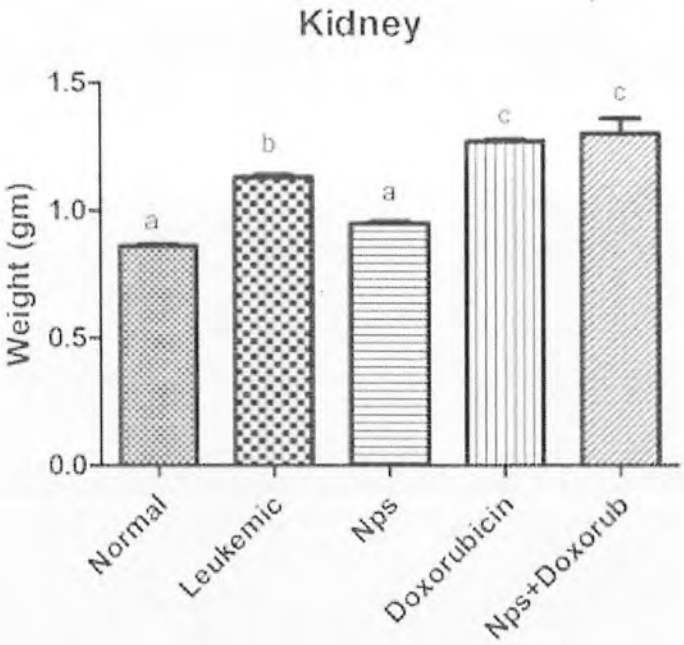

Figure 3.8 Relative organ weights of kidney in different treated groups

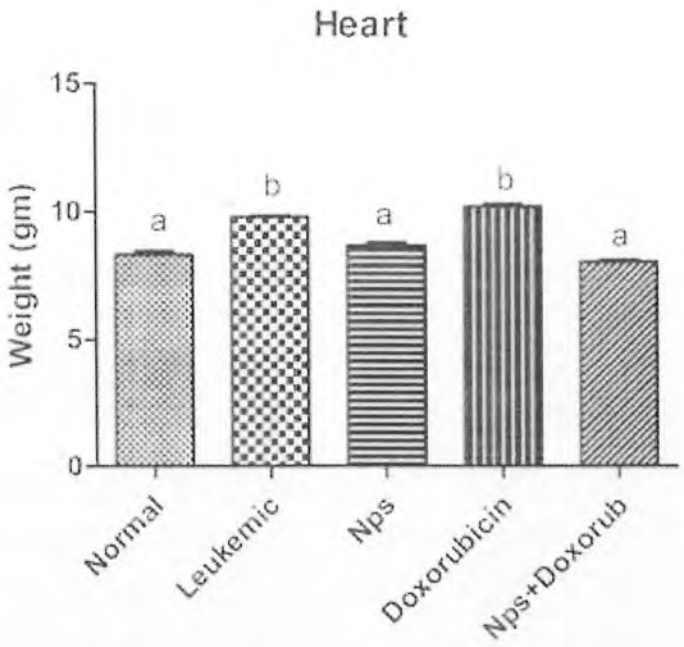

Figure 3.9Relative organ weights of heart in different treated groups

3.10 Complete Blood Count

To examine the effects of different drug and nanoparticle combinations upon blood cells count, complete blood count was obtained.

3.11 White Blood Cells

White blood cells were counted and analyzed by complete blood picture. It was observed that the total WBCs count was significantly increased in group 2 which is a sign of myeloid leukemia. The abnormal increase was restored in CeO_2 nanoparticles doxorubicin and nanomedicine .These groups have significantly decreased WBCs count just like those as in control group as inferred from statistics ($p<0.05$).

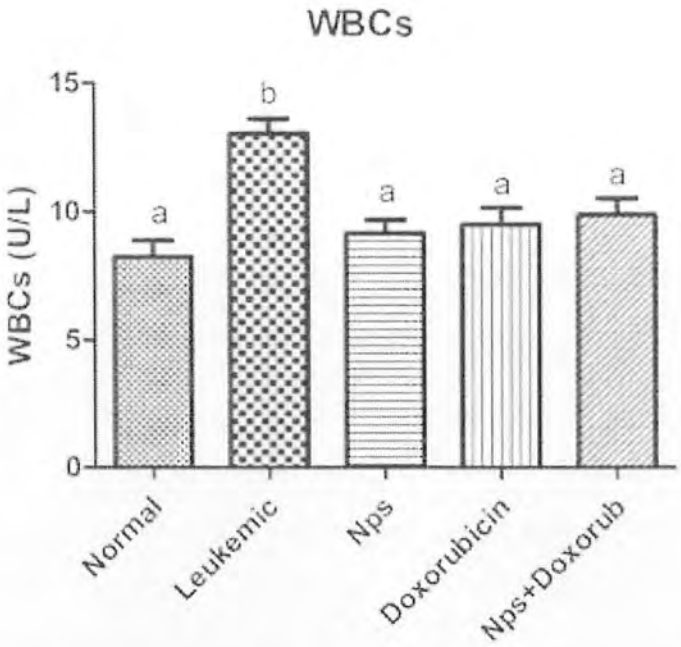

Figure 3.11 Comparison of total WBCs count in different treated groups

3.12 Red Blood Cells

It was observed that the total red blood cells count was significantly decreased after the treatment with benzene ($P<0.05$). Upon treatment with nanoparticles i.e. group 3 red blood cells was not significantly increased. Doxorubicin and nanomedicine treated groups also did not cause a significant increase in red blood cells.

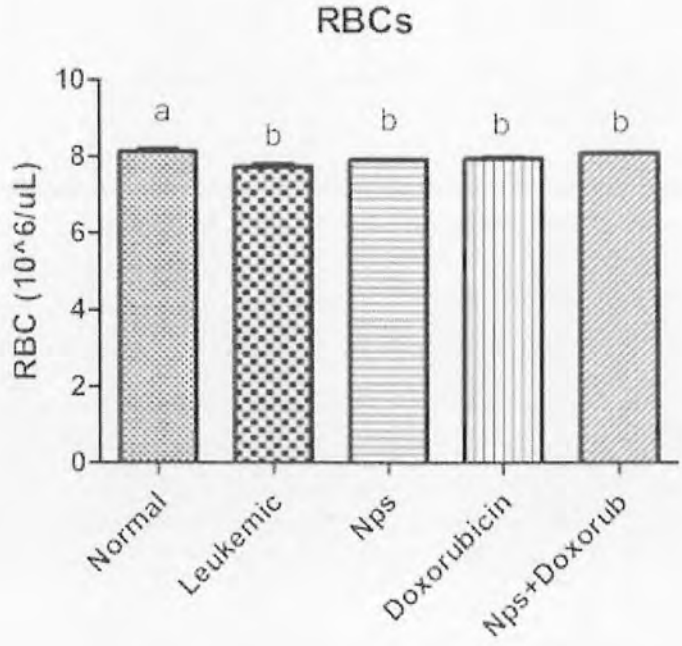

Figure 3.12Comparison of total RBCs count in different experimental groups

3.13 Monocytes

From the complete blood count it was observed that the monocytes were significantly increased upon benzene treatment. A significant decreased was observed after treating with nanoparticles and nanomedicine as group 3 and 5 recovered the monocytes to normal. But in doxorubicin treated group there was no significant decrease in monocytes count.

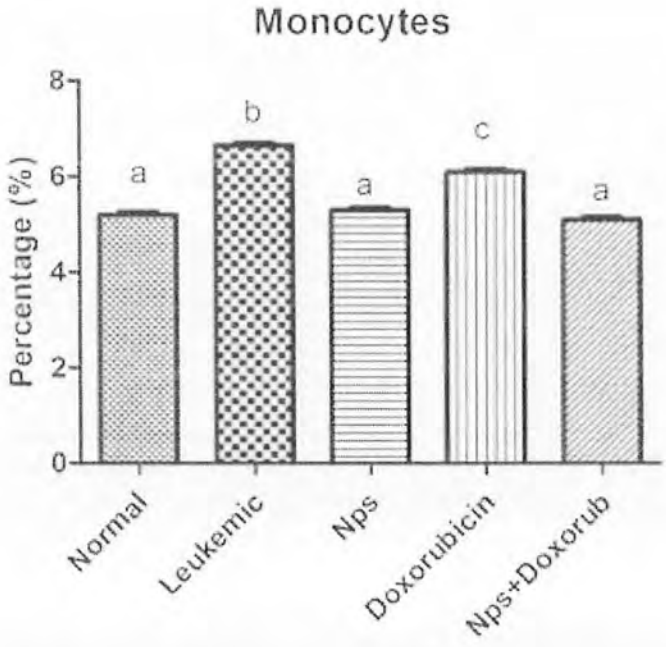

Figure 3.13 Comparison of totalmonocytes count in different groups

3.14 Eosinophils

A significant increase in eosinophils count was observed in benzene treated rats. However no significant difference was observed after treatment with the nanoparticles. But treatment with doxorubicin and combination of nanoparticles and doxorubicin showed a significant decrease in eosinophils count ($p<0.05$).

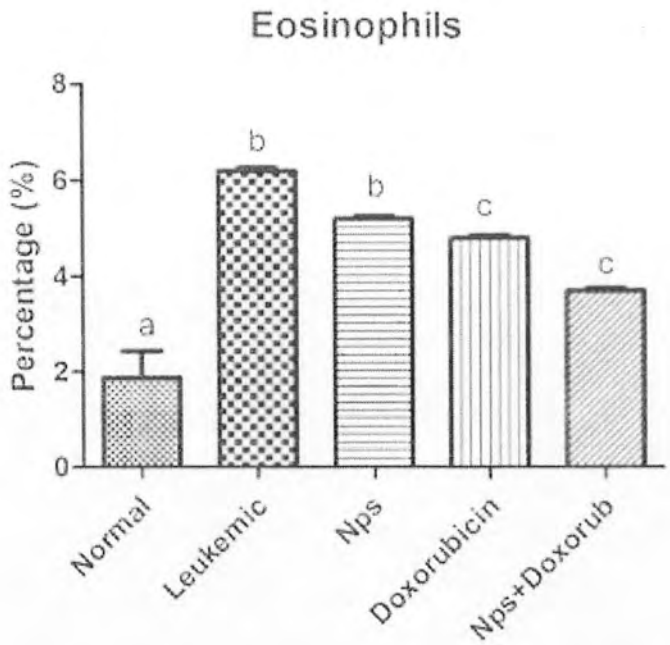

Figure 3.14 Comparison of eosinophils count in different experimental groups

3.15 Neutrophils

From the complete blood picture it was found that neutrophils count increased in benzene treated rats. Treatment with nanoparticles significantly reduced the neutrophils count in group 3 treated rats. Treatment with doxorubicin also reduced the levels of neutrophils count. However, the co-administration of doxorubicin and nanoparticles did not cause a significant reduction in neutrophils count.

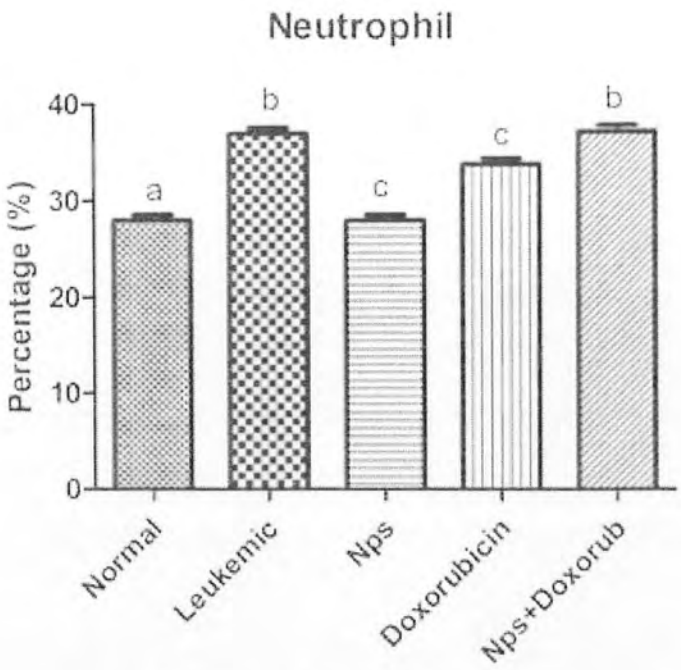

Figure 3.15 Comparison of neutrophils count in different experimental groups

3.16 Lymphocytes

It was observed that the absolute lymphocytes count increased in benzene treated rats. Nanoparticles exhibited much reduced levels of lymphocytes count. Such effect was also observed in doxorubicin and nanomedicine treated groups. Groups 3, 4 and 5 had significantly decreased levels of lymphocytes count as compared to leukemic group ($p<0.05$).

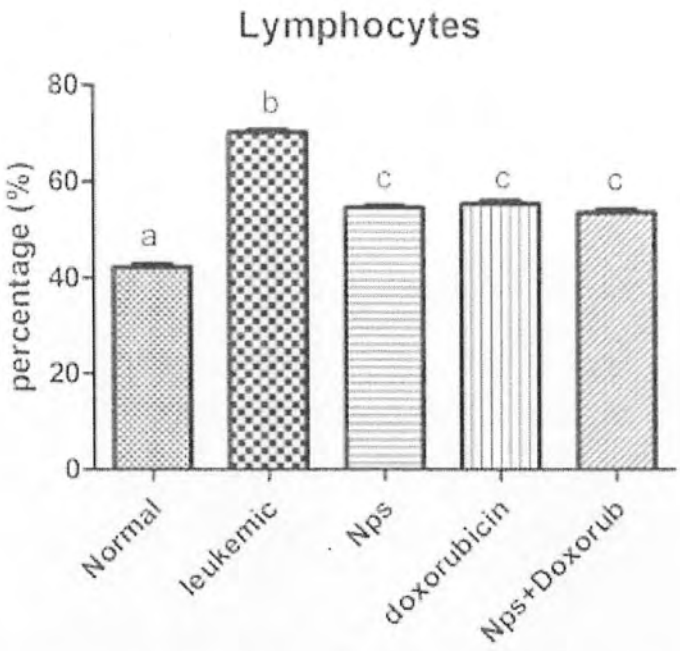

Figure 3.16Comparison of lymphocytes count in different experimental groups

3.17 Haemoglobin

The haemoglobin levels decreased slightly in benzene treated group. There was a significant difference between leukemic and nanoparticles and doxorubicin treated groups. The groups 3, 4 and 5 had significantly increased levels of haemoglobin as compared to group 2 i.e. leukemic group ($p<0.05$).

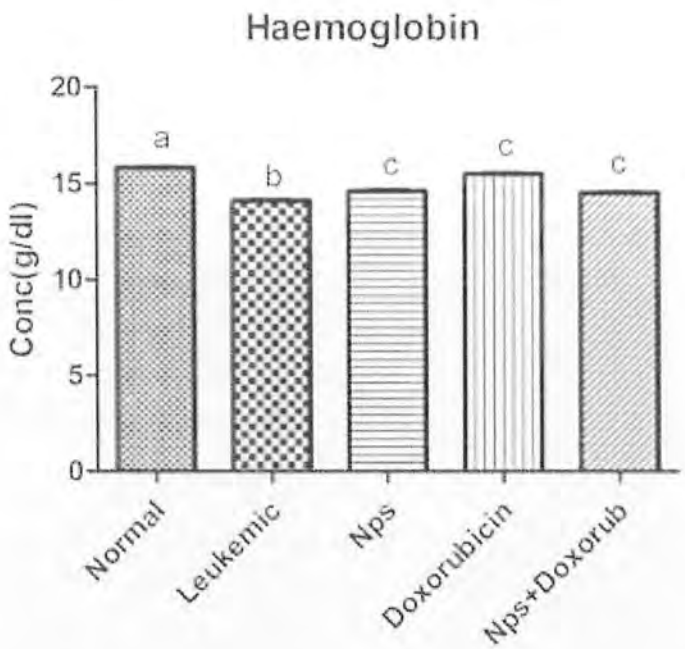

Figure 3.17 Comparison of haemoglobin levels in different experimental groups

3.18 Annexin V Binding Assay

Annexin V binding assay was performed for the detection of apoptotic cells. In this quadrant graph, on x-axis we have Annexin V fluorescence and on y-axis propidium iodide fluorescence. On the right hand side the cells are positive for Annexin V and it indicates the early and late apoptosis. On the left hand side the cells indicate the live and dead cells. Healthy cells are negative for propidium iodide and Annexin V.

In case of normal group 1 (graph a) rats the total gated events were 1090 of which the live cells were 976, dead cells were 71, no early apoptotic cells were found and 43 late apoptotic cells. In case of leukemic group 2 (graph b) the total gated events were 995 of which the live cells were 190, 32 dead cells, 77 early apoptotic cells and 656 are late apoptotic cells. The group 3 nanoparticles (graph c) treated group total gated events were 826 of which 214 live cells, 99 dead cells, 86 early and 427 were late apoptotic cells. In doxorubicin treated group (graph d) the total gated events were 951 of which 300 were live cells, 87 dead, 187 early apoptotic and 446 late apoptotic cells. The total gated events in nanomedicine treated group (graph e)were 1420, live cellswere 494, early apoptotic cells 183, late apoptotic cells 647 and dead cells were 96. The details are shown in Table 3.3.

Table 3.3 Annexin V Flow Cytometry Results

Sr. No	Sample	Total Gated Events	Live Cells	Dead Cells	Early Apoptotic cells	Late apoptotic cells	Total
1	Normal	1090	976	71	0	43	43
2	Leukemic	955	190	32	77	656	733
3	CeO_2	826	214	99	86	427	513
4	Doxorubicin	951	300	87	118	446	564
7	CeO_2+doxo	1420	494	96	183	647	830

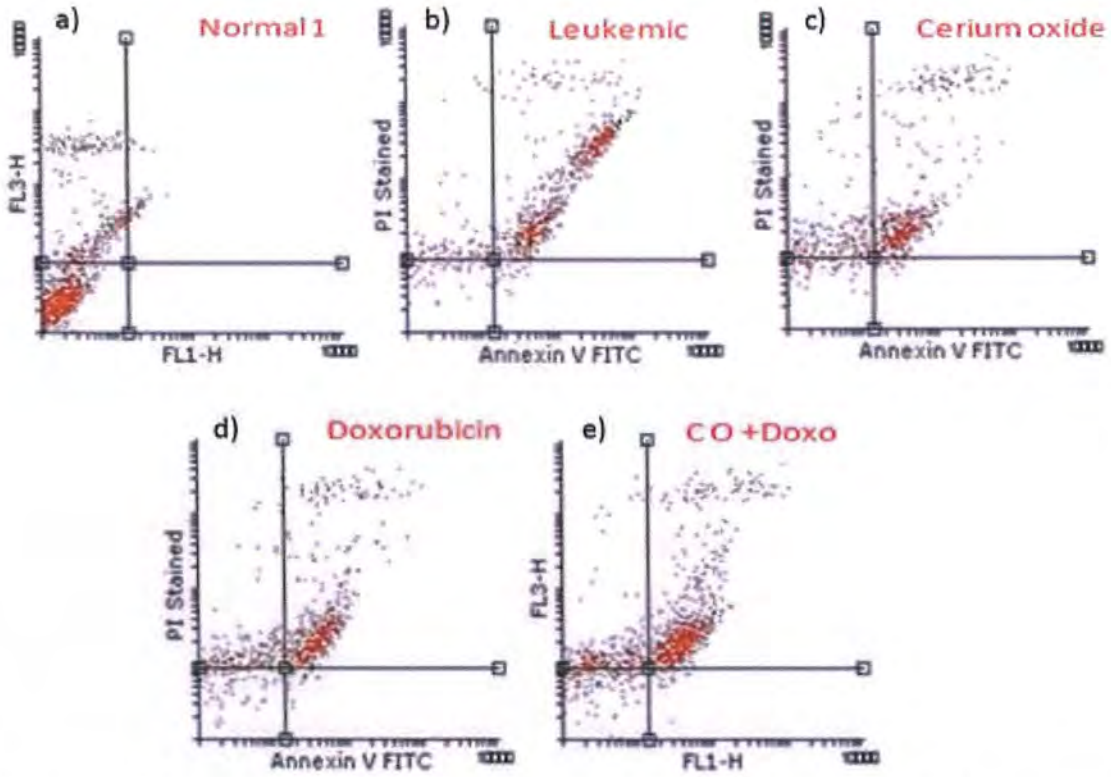

Figure 3.18 Graphs showing apoptosis in (a) Normal (b) Leukemic (c) CeO_2 (d) Doxorubicin (e) CeO_2+doxorubicin groups

3.19 Microscopic Examination of Blood Cells

Slides were stained with Giemsa dye after fixing with chilled methanol. Figure 3.6(a) represents normal blood cells with well defined morphology and (b) shows leukemic cells having large number immature white blood cells or blast cells.

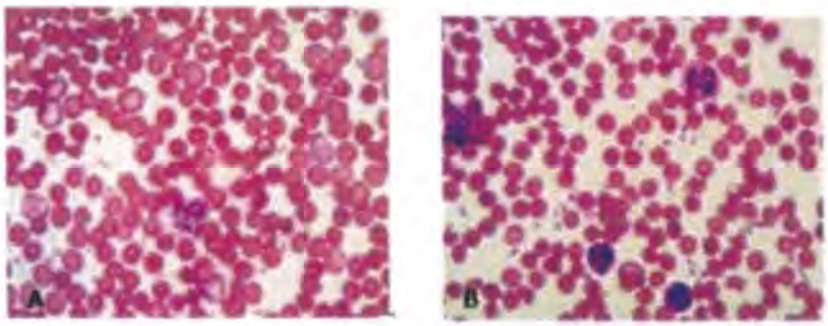

Figure 3.19 Microscopic examination of blood cells of (a) Normal (b) Leukemic

3.20 Biochemical Assessment

3.21 Estimation of Hepatic Biomarkers

Biochemical evaluation of hepatic biomarkers revealed following results.

A) Alkaline Phosphatase (ALP)

A significant decrease was seen in ALP levels in case of benzene treated rats as compared to normal rats. Treatment with nanoparticles showed recovery in serum ALP levels in case of group 3 ($p<0.05$). Doxorubicin and the doxorubicin in conjugation exhibited more enhanced serum ALP levels as compared to normal.

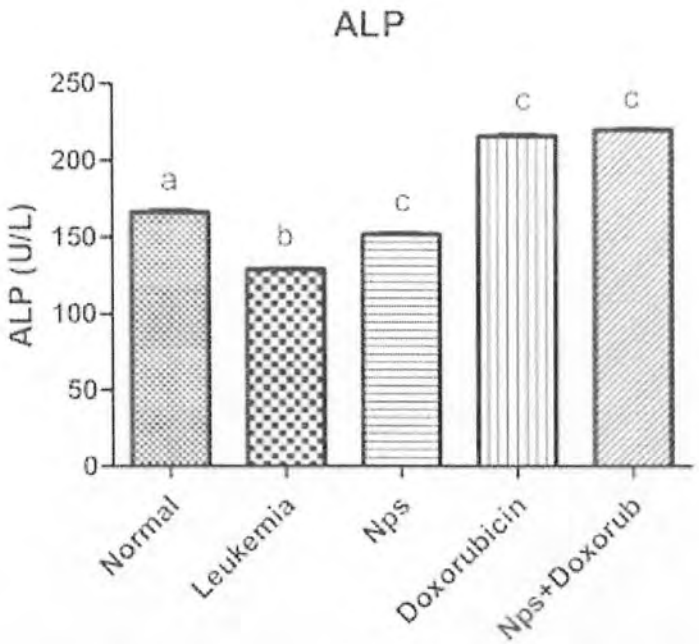

Figure 3.23 Comparison of serum ALP levels in different experimental groups

b) Alanine Transferase (ALT)

It was observed that the ALT levels increased significantly in leukemic group as compared to the control. However this increase was significantly reduced by treatment with nanoparticles. Treatment with doxorubicin or nanomedicine did not cause a significant decrease in ALT levels.

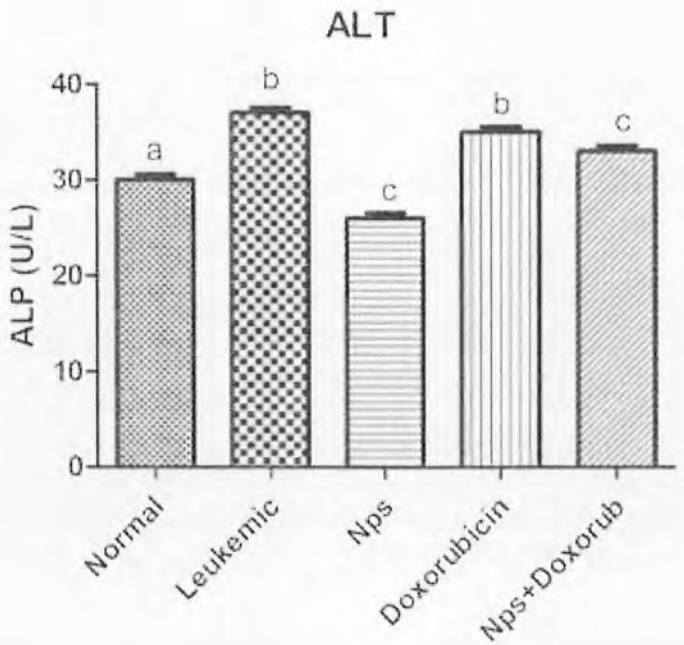

Figure 3.24 Comparison of serum ALT levels in different experimental groups

c) Aspartate Transferase (AST)

Control and leukemic groups represented normal and benzene treated rats, respectively. A significant increase in serum AST levels in benzene treated rats was observed as compared to normal group. However these enhanced expression levels were reduced in nanoparticles treated group ($p<0.05$). But in case of group 4 and 5 the AST levels were very high.

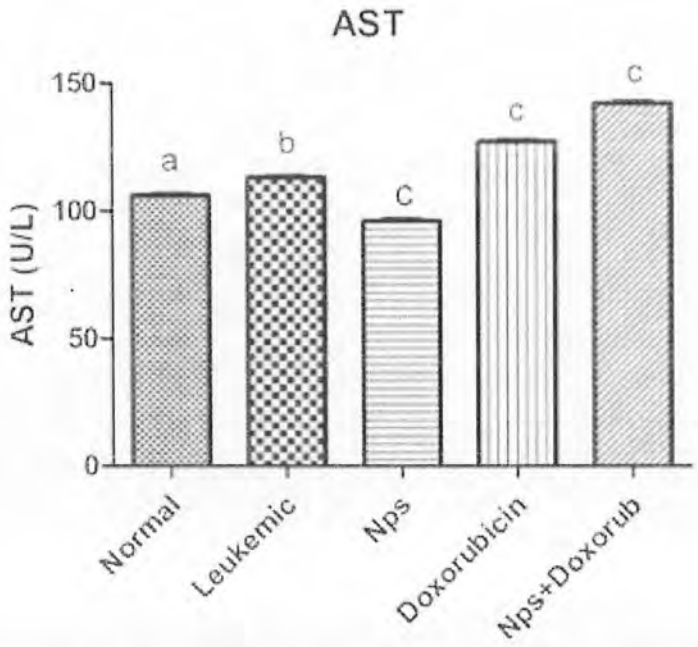

Figure 3.25 Comparison of Serum AST levels in different experimental groups

3.26Estimation of Renal Biomarkers

3.2.1 Urea

By measuring urea levels, it was observed that the benzene treated rats have significantly increased levels of urea as compared to normal. Group 3 which was treated with the CeO_2 nanoparticles had significantly increased urea levels as compared to leukemic group. Doxorubicin showed no significant results as compared to leukemic group. The nanomedicine showed similar results to those of nanoparticles i-e significantly increased levels of urea.

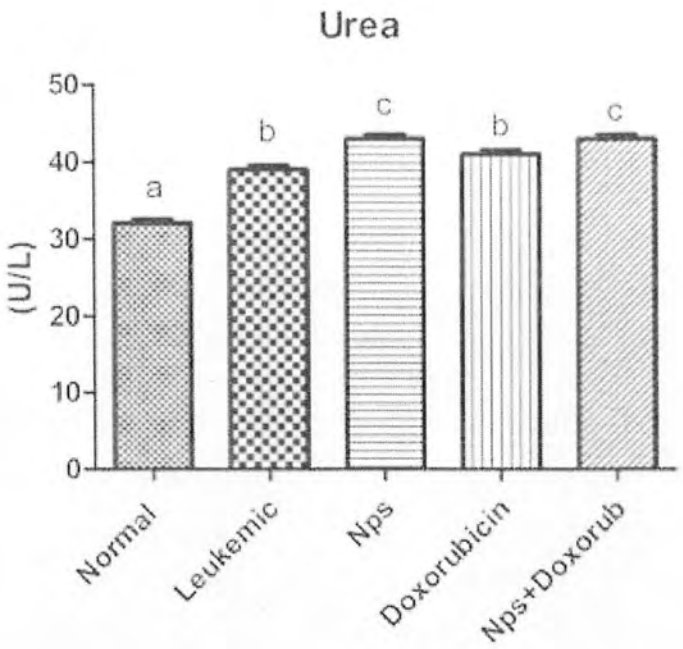

Figure 3.26Serum urea levels of different experimental groups

3.27 Blood Urea NitrogenTest

Blood Urea Nitrogen (BUN) test was performed to evaluate kidney function. It was performed to find out urea nitrogen levels in the blood. The group 2 leukemic group had significantly increased BUN levels as compared to normal group. There was no statistical decrease in BUN levels in group 3, 4 and 5.

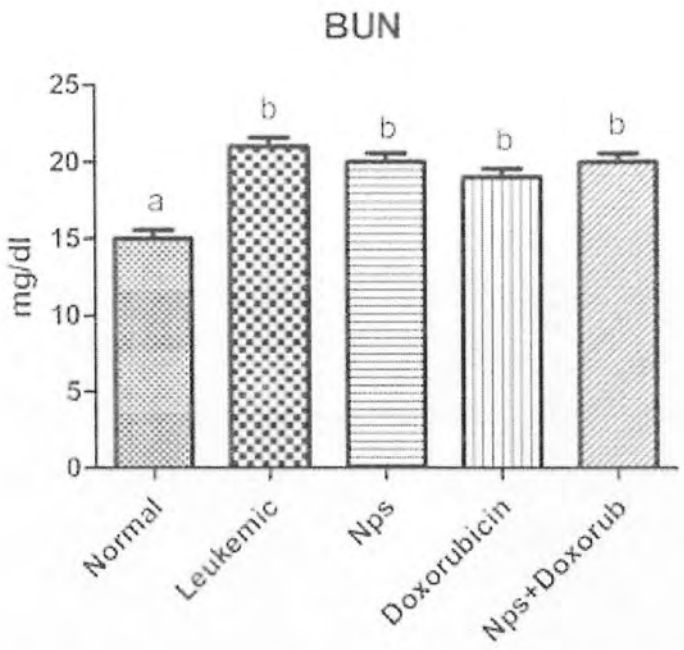

Figure 3.27 Estimation of BUN levels in different experimental groups

3.28 Creatinine C

By using renal biomarkers against creatinine C levels, it was observed that the creatinine levels were significantly increased in group 2 i.e. benzene administered rats. Nanoparticles treated group i.e. group 3 had significantly reduced creatinine levels near to normal values. But in case of doxorubicin no decrease in creatinine levels was observed. The nanomedicine treated group had significantly decreased levels of creatinine as compared to leukemic group ($p<0.05$).

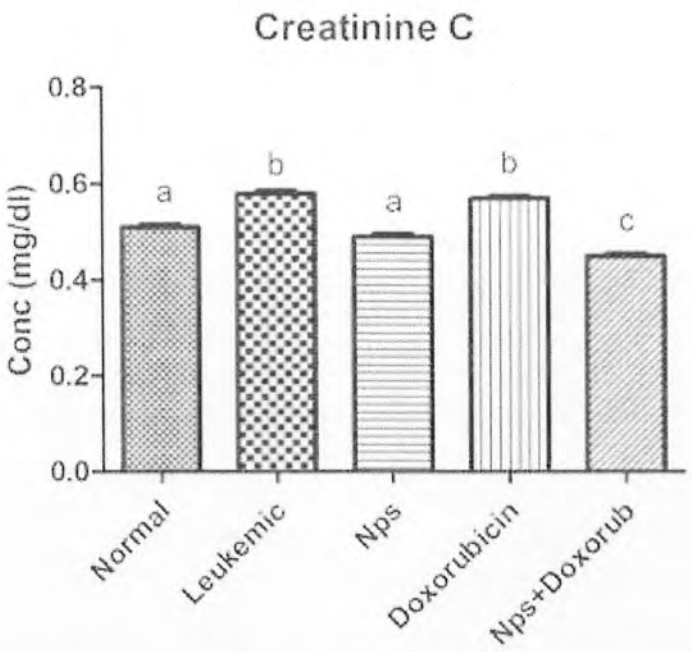

Figure 3.28 Estimation of creatinine levels in different experimental groups

3.29 Real Time PCR

For relative gene expression analysis quantitative Real Time PCR was performed.

3.30 Relative Expression Analysis

a) p53

By using qPCR relative expression analysis technique, it was observed that the expression of the p53was significantly decreased in benzene treated rats i.e. leukemic group. The expression of p53 remained low by treatment with nanoparticles and nanomedicine.Treatment with doxorubicin showed some increase in p53 levels but it was not significant ($p<0.05$).

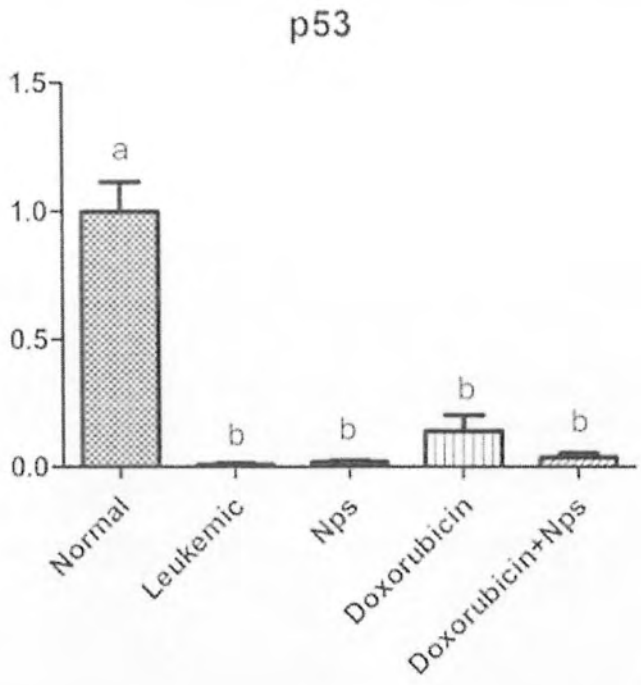

(a)

Figure 3.30 Relative expression analysis of p53 in different experimental groups

b) Rel A

RT PCR revealed a significant decrease in the expression analysis of Rel A in benzene treated ratsi.e. group 2. However a significant increase was seen in Rel A expression in group 3 which was nanoparticles treated group. Alow expression of Rel A was observed in group 4 and group 5 rats.

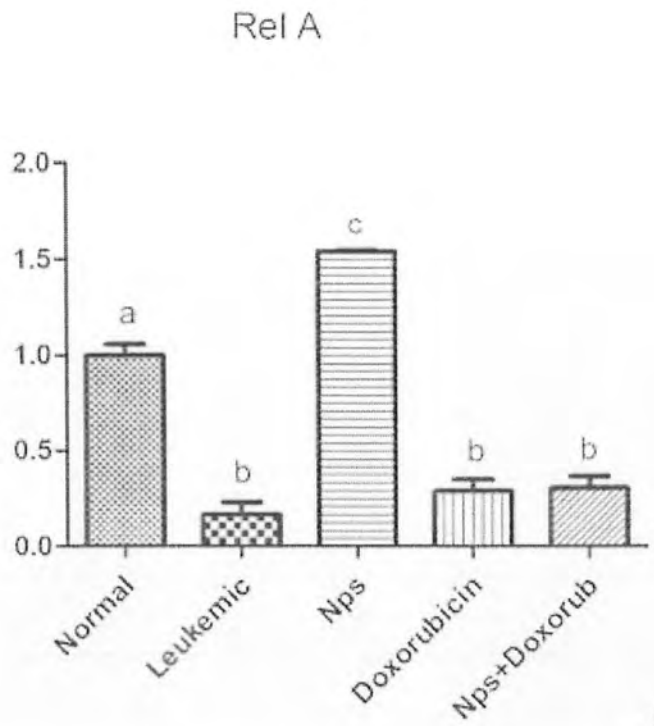

(b)

Figure 3.31Relative expression analysis of Rel A in different experimental groups

c) Rel B

RT analysis showed increased levels of Rel B in benzene treated rats i.e. group 2. But upon treatment with nanoparticles, doxorubicin and nanomedicine,the Rel B was decreased.

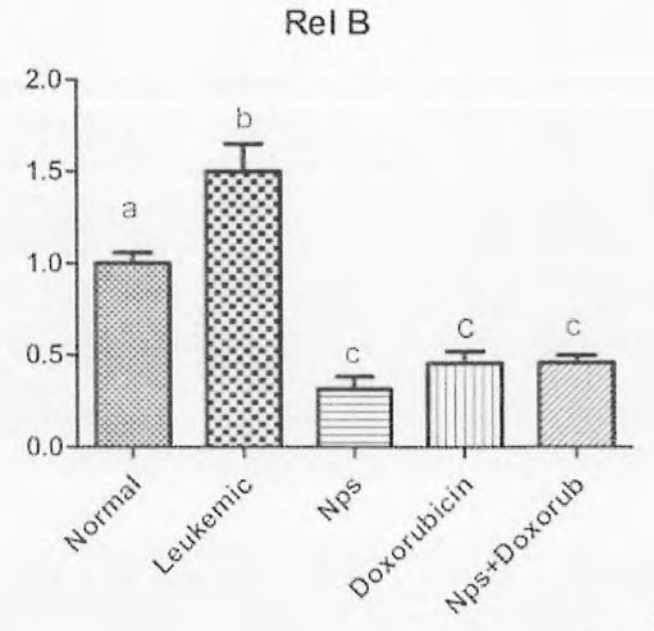

(c)

Figure 3.32 Relative expression analysis of Rel B in different experimental groups

d) STMN 1

Stathmin 1 plays a significant role in the cell motility, survival and cell progression. The STMN 1 was not up regulated in leukemic group. The expression of STMN 1 was not significantly increased in any of the groups and it remained down regulated in all groups.

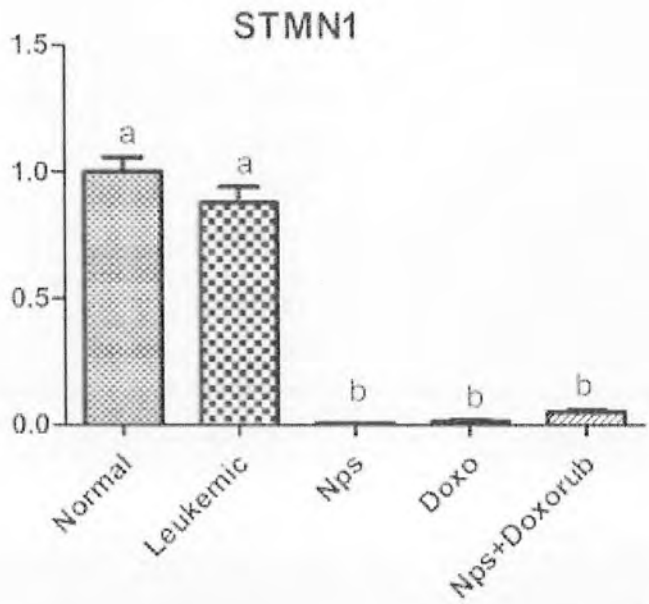

(d)

Figure 3.33 Expression of STMN 1 in different groups

e) Cytochrome C

RT PCR revealed a significant decrease in the expression analysis of the Cytochrome c in group 2 i.e. benzene treated rats. However,the expression was almost restored upon treatment with doxorubicin. Nanoparticles and nanomedicine did not show much ability to restore Cytochrome c levels in leukemic rats.

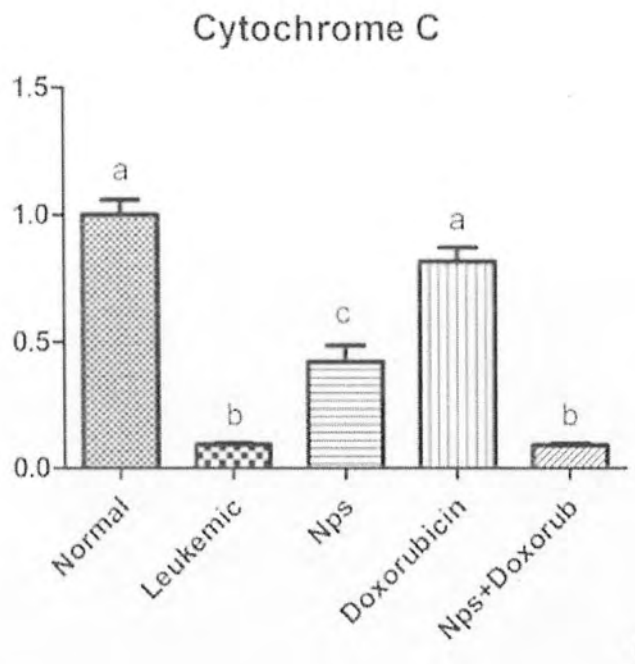

(e)

Figure 3.34 Relative expression analysis of Cytochrome c in different experimental groups

f) Caspase 3

The RT expression analysis showed the decreased expression of caspase 3 in group 2 i.e. benzene treated group. In group 3 i.e. nanoparticles treated group, there was a significant increase in caspase 3 expression. The expression of caspase 3 was found to be down regulated in group 4 and group 5 ($p<0.05$).

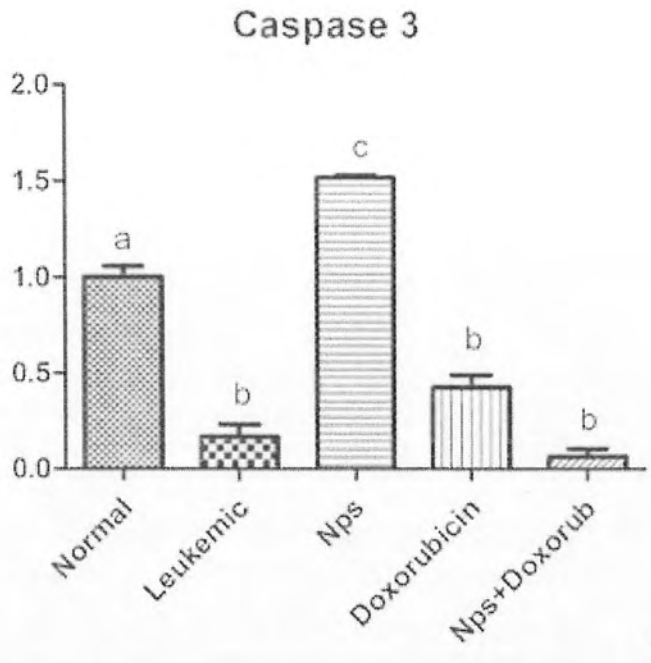

(f)

Figure 3.35 Relative expression analysis of caspase 3 in different experimental groups

g) Caspase 9

RT analysis showed increased expression of Caspase 9 in benzene treated group. There was a further up regulation of caspase 9 in nanoparticles treated group. Caspase 9 was also upregulated in group 4. But it was restored to normal in the nanomedicine treated group 5.

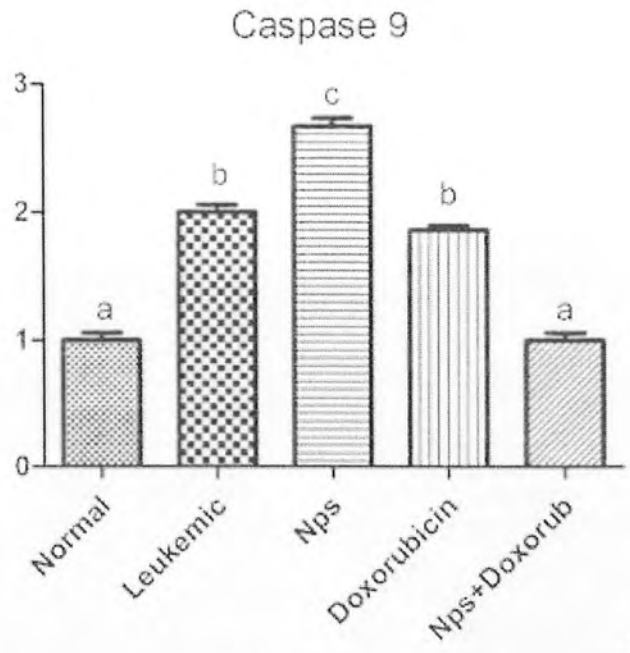

(g)

Figure 3.36 Relative expression analysis of Caspase 9 in different experimental groups

h) Bax

RT analysis of bax showed decreased expression of bax in benzene treated rats i.e. group 2. Upon treatment with nanoparticles and doxorubicin the expression of bax was improvedas compared to leukemic group. The expression of the bax in nanomedicine treated group was similar to normal group ($p<0.05$).

5. References

Alili, L., Sack, M., Karakoti, A. S., Teuber, S., Puschmann, K., Hirst, S. M.& Seal, S. (2011). Combined cytotoxic and anti-invasive properties of redox-active nanoparticles in tumor–stroma int eractions. *Biomaterials*, *32*(11), 2918-2929

Arnold, M., Soerjomataram, I., Ferlay, J., & Forman, D. (2015). Global incidence of oesophageal cancer by histological subtype in 2012. *Gut*, *64*(3), 381-387.

Ashkenazi, A. (2002). Targeting death and decoy receptors of the tumour-necrosis factor superfamily. *Nature Reviews Cancer*, *2*(6), 420.

Ashkenazi, A. (2008). Targeting the extrinsic apoptosis pathway in cancer. *Cytokine &Growth Factor Reviews*, *19*(3-4), 325-331.

Bennett, J. M., Catovsky, D., Daniel, M. T., Flandrin, G., Galton, D. A. G., Gralnick, H. R., & Sultan, C.(1982). Proposals for the classification of the myelodysplastic syndromes. *British journal of haematology*, *51*(2), 189-199.

Boyland, E. (1952). Different types of carcinogens and their possible modes of action: a review. *Cancer Research*, *12*(2), 77-84.

Cappetta, D., Rossi, F., Piegari, E., Quaini, F., Berrino, L., Urbanek, K., & De Angelis, A. (2018). Doxorubicin targets multiple players: a new view of an old problem. *Pharmacological Research*, *127*, 4-14.

Caputo, F., De Nicola, M., Sienkiewicz, A., Giovanetti, A., Bejarano, I., Licoccia, S.,& Ghibelli, L. (2015). Cerium oxide nanoparticles, combining antioxidant and UV shielding properties, prevent UV-induced cell damage and mutagenesis. *Nanoscale*, *7*(38), 15643-1

Cardinale, D., Colombo, A., Lamantia, G., Colombo, N., Civelli, M., De Giacomi, G., & Cipolla, C. M. (2010). Anthracycline-induced cardiomyopathy: clinical relevance and response to pharmacologic therapy. *Journal of the American College of Cardiology*, *55*(3), 213-220.

Celardo, I., De Nicola, M., Mandoli, C., Pedersen, J. Z., Traversa, E., & Ghibelli, L. (2011). Ce3+ ions determine redox-dependent anti-apoptotic effect of cerium oxide nanoparticles. *ACS Nano*, *5*(6), 453

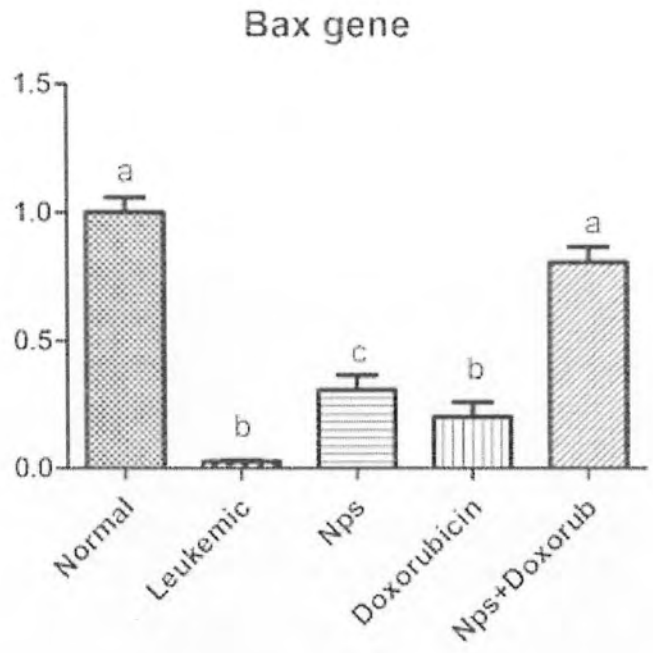

(h)

Figure 3.37Relative expression analysis of bax in different experimental groups

i) Caspase 8

RT analysis of caspase 8 showed that caspase 8 was slightly down regulated in groups 2, 3 and 4. But in nanomedicine treated group the expression of caspase 8 was exponantially up regulated as compred to all the experimental groups.

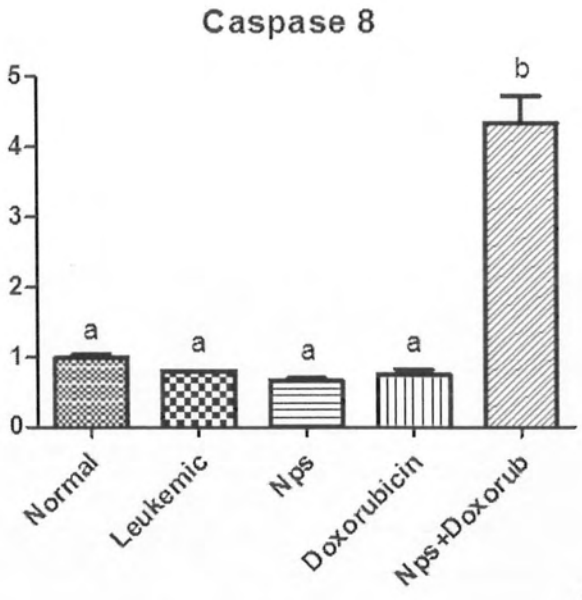

(i)

Figure 3.38 Relative expression of caspase 8 in different experimental groups

4. Discussion

Doxorubicin belongs to anthracyclines and is one of the broadly used chemotherapeutic drugs utilized for the treatment of several malignancies such as leukemia, lymphoma and sarcoma. Hepatic, cardiac and renal toxicity are the systemic side effects of doxorubicin which restricts the usage of thismedication (Wang *et* al., 2015). Nanotechnology is largely used to improve therapeutic approach against cancer and nanoparticles have been reported to have such pharmacokinetic and pharmacodynamic properties that increase their efficiency with less toxicity (Wiski *et* al., 2015).

Nanoparticles can cross cell membrane and can cross blood-brain-barriers to overcome the main hindrance of site specific delivery, which significantly lessens off-target side effects. Cerium Oxide belongs to rare earth metal oxides and possesses exclusive property to switch between Ce^{3+} and Ce^{4+} according to the environment (Estevez and Erlichman, 2014). Keeping in view the above mentioned points, we have developed a cerium oxide based drug delivery system for treating leukemic rats.

Before using the nanoparticles for our study, we confirmed its size and other properties. The XRD pattern confirmed the particle size of the nanoparticles was 14.7 nm (figure 3.1). The particle size is an essential factor in determining the cellular interaction, rate of activity and sub cellular distribution (Xu and Qu, 2014). So, a particle size less than 30nm was recommend to utilize to enhance the percentage of Ce^{+3} valence states (Nelson *et al.,* 2016). After confirming the size, the charge on the nanoparticles was found by zeta potential and nanoparticles were found to be slightly negative (figure 3.2). The cationic anticancer drug was loaded on the CeO_2 nanoparticles by simple electrostatic interaction for *in vivo* drug delivery to leukemic rats (Das *et al.*, 2017). The adsorption of the doxorubicin on the surface of the Cerium Oxide nanoparticles was established by UV-Vis and FTIR analysis. The change of the color of doxorubicin from red to pink confirms the loading of drug on nanoparticles. The FTIR analysis showed the multiple characteristics peaks, the broad peak at 3260 cm^{-1} showed the C-H stretch and aromatics showed C-H stretch. The peaks at 1635 cm^{-1} are due to banding band of N-H groups (Chen *et al.,* 2015). The stretching of the peaks showed the loading of the drug (figure 3.1.3).

In the present study, as benzene is a potent inducer of AML so benzene was administered intraperitoneally on every alternate day for three weeks, resulting in Acute Myeloid Leukemia.

After 14 days of benzene treatment, hematological profiling of rats, which could be due to the severity of the disease, deteriorated as confirmed by already published data (d' Azevedo *et* al., 1996). The AML was confirmed by examining blood cells morphology and count. It was observed that in benzene treated rats the number of the blast cells or immature white blood cells was increased and red blood cells shape was also ruptured. Complete blood count revealed that the total WBCs count increased significantly due to the presence of the blast cells or immature leukocytes in blood. Treatment of the rats with nanoparticles, doxorubicin and nanomedicine significantly reduced the total WBCs count showing the anti-leukemic potential of Cerium Oxide nanoparticles which has not been reported before. Likewise the levels of absolute monocytes, lymphocytes, eosinophils was increased in leukemic rats indicating the induction of AML .The increase in lymphocytes in benzene treated rats is an indicator of AML. The treated groups had significantly reduced levels of lymphocytes in groups 3, 4 and 5. The alteration in the blood cells count confirms AML, also reported in already published data (D Andrea and Reddy, 2014). During the diagnosis of acute myeloid leukemia the increased number of lymphocytes is associated with a shorter remission (Mussai *et al.*, 2013).

Next we investigated the relative weights of liver, heart and kidney and found them to be significantly increased in group 2 i.e. leukemic group indicating hypertrophy of the organs. In case of the liver, benzene is known to cause hypertrophy (Roy, 2016).The treatment with nanoparticles and nanomedicine decreased the weight near to normal. The doxorubicin did not cause decrease in organs weight as 40% of the patients taking doxorubicin have affected liver function as reported in already published data (Damodar *et al.*, 2014). Oxidative stress, apoptosis and interference with the electron transport chain could be the cause of the hepatic toxicity from doxorubicin (Jung *et al.*, 2014). In case of kidney weight, the nanoparticles showed decrease in weight but nanomedicine did not show decrease in weight. In case of heart the nanoparticles and nanomedicine significantly reduced the weight but doxorubicin did not show any significant decrease in weight. The results are in line with already published data

which showed a significant increase in relative liver and kidney weight of the rodents treated with doxorubicin as compared to the normal group (Herman *et al.*, 2000).

In this research work, cerium oxide came out with promising anti cancerous activity. To check that whether the nanoparticles and nanomedicine cause apoptosis, Annexin V assay was performed. The leukemic group had large number of apoptotic cells. These results are in line with already published data where a large number of evidence has shown that benzene and its metabolites cause apoptosis in multiple cell types (Chow *et al.*, 2015; Huang *et al.*, 2015; Xu *et al.*, 2017). Nuclear localization of β-catenin and LEF-1 are inhibited by hydroquinone treatment and that's why downstream transcriptional responsive genes such as Survivan and Cyclin D1 are inhibited which otherwise promote cell cycle and cell proliferation (Li *et al.*, 2018).

The above data suggest possible potential of CeO_2 in treatment of leukemia. These findings were confirmed further by biochemical assessment of hepatic biomarkers (ALT, AST and ALP) in serum of rats. Results showed significant increase in levels of AST and ALT while significant decrease in ALP levels in response to benzene administration which corresponded to already published data (d'Azevedo *et al.*, 1996; Dere and Ari, 2009). The reduced levels of ALP enzymatic activity in benzene treated rats is because of lack of the detectable LAP (Leukocyte Alkaline Phosphatase) mRNA in AML, whereas elevation in ALT levels is due to abnormal proliferation of liver cells leading to increased Alanine transaminases in leukemic rats.

Interestingly, qPCR expression analysis showed the down regulated expression of p53 in leukemic group. p53 a tumor suppressor protein is either by mutation or dysregulation is inactivated in a large number of cancers, by disturbing the nucleo-cytoplasmic shuttling of p53 or by means of induction of the p53 inhibitor MDM2. In AML the dysregulation of p53 function come out as frequent event (Columbo *et al.*, 2002). p53 is found to be down regulated in acute myeloid leukemia, leukemic cell lines and myeloproliferative diseases (Prokocimer *et al.*,1986).Detectable levels of p53 mRNA are not expressed by numerous myeloid leukemias and by a large number of breast cancer cell lines (Durland and Reisman, 2002).

To figure out NF-kappa B signaling pathway the relative expression of Rel A was checked and was found to be significantly lower in benzene treated rats. This is probably one of the mechanisms through which benzene causes cell death i.e. by

interfering in the cell survival mechanism mediated through NF-kappa B. But it was high in nanoparticles treated group. The expression of Rel B which belongs to non-canonical pathway, was up regulated in leukemic group potentially linked to increased survival and proliferation of transformed cells. The already reported data showed that cell survival and apoptosis two of the important processes are regulated by NF-kappa B pathway (DeGraffenried *et al.*, 2004).

The qPCR expression of caspase 3 and caspase 9 showed immense up regulation in response to nanoparticles. Both these genes are responsible for execution of apoptosis and these results point towards the absolute potential of Cerium Oxide nanoparticles towards apoptosis.In addition, our nanoparticles show a significant role in Cytochrome c production which is another apoptosis inducer. These results were according to the already reported data that claimed CeO_2 totrigger apoptosis of the cancer cells by releasing Cytochrome c and activating Caspase 3 and 9 and thereby, initiating mitochondrial signaling pathway (Wang *et al.*, 2013)

Conclusion

It is concluded that cerium oxide nanoparticles alone or in combination with doxorubicin showed substantial therapeutic potential against AML in rat model. It has the ability to minimize the effects of benzene induced leukemia as proven by differential leukocyte counts, relative organ weight analysis, estimation of hepatic biomarkers and relative gene expression.

Celardo, I., Pedersen, J. Z., Traversa, E., & Ghibelli, L. (2011). Pharmacological potential of cerium oxide nanoparticles. *Nanoscale*, *3*(4), 1411-1420.

Chen, G. Q., Zhu, J., Shi, X. G., Ni, J. H., Zhong, H. J., Si, G. Y., ... & Shen, Z. X. (1996). In vitro studies on cellular and molecular mechanisms of arsenic trioxide (As2O3) in the treatment of acute promyelocytic leukemia: As2O3 induces NB4 cell apoptosis with downregulation of Bcl-2 expression and modulation of PML-RAR alpha/PML proteins. *Blood*, *88*(3), 1052-1061.

Chen, L., Xue, Y., Xia, X., Song, M., Huang, J., Zhang, H., ... & Huang, S. (2015). A redox stimuli-responsive superparamagnetic nanogel with chemically anchored DOX for enhanced anticancer efficacy and low systemic adverse effects. *Journal of Materials Chemistry B*, *3*(46), 8949-8962.

Chow, P. W., Hamid, Z. A., Chan, K. M., Inayat-Hussain, S. H., & Rajab, N. F. (2015). Lineage-related cytotoxicity and clonogenic profile of 1, 4-benzoquinone-exposed hematopoietic stem and progenitor cells. *Toxicology and Applied Pharmacology*, *284*(1), 8-15.7-4549.

Conesa, J. (1995). Computer modeling of surfaces and defects on cerium dioxide. *Surface Science*, *339*(3), 337-352.

Cui, N., Hu, M., & Khalil, R. A. (2017). Biochemical and biological attributes of matrix metalloproteinases. In *Progress in Molecular Biology and Translational Science* (Vol. 147, pp. 1-73). Academic Press.

D'Andrea, M. A., & Reddy, G. K. (2014). Hematological and hepatic alterations in nonsmoking residents exposed to benzene following a flaring incident at the British petroleum plant in Texas City. *Environmental Health: A Global Access Science Source*, *13*(1), 1–8.

Das, J., Choi, Y. J., Han, J. W., Reza, A. M. M. T., & Kim, J. H. (2017). Nanoceria-mediated delivery of doxorubicin enhances the anti-tumour efficiency in ovarian cancer cells via apoptosis. *Scientific Reports*, *7*(1), 9513.

Das, S., Dowding, J. M., Klump, K. E., McGinnis, J. F., Self, W., & Seal, S. (2013). Cerium oxide nanoparticles: applications and prospects in nanomedicine. *Nanomedicine*, *8*(9), 1483

DeGraffenried, L. A., Chandrasekar, B., Friedrichs, W. E., Donzis, E., Silva, J., Hidalgo, M.,& Weiss, G. R. (2004). NF-κB inhibition markedly enhances sensitivity of resistant breast cancer tumor cells to tamoxifen. *Annals of Oncology*, *15*(6), 885-890.1508.5656.

Dere, E., & Ari, F. (2009). Effect of benzene on liver functions in rats (Rattus norvegicus). *Environmental Monitoring and Assessment*, *154*(1–4), 23–27.

DeSantis, C. E., Fedewa, S. A., Goding Sauer, A., Kramer, J. L., Smith, R. A., & Jemal, A. (2016). Breast cancer statistics, 2015: Convergence of incidence rates between black and white women. *CA: ACancer Journal for Clinicians*, *66*(1), 31-42.

DeSantis, C. E., Lin, C. C., Mariotto, A. B., Siegel, R. L., Stein, K. D., Kramer, J. L., ... & Jemal, A. (2014). Cancer treatment and survivorship statistics, 2014. *CA: ACancer Journal for Clinicians*, *64*(4), 252-271.

DeVita, V. T., Lawrence, T. S., & Rosenberg, S. A. (2012). *Cancer: principles & practice of oncology: primer of the molecular biology of cancer*. pp 114-127, China: Library of Congress Catalonging in Publication Data

Döhner, H., Weisdorf, D. J., & Bloomfield, C. D. (2015). Acute myeloid leukemia. *New England Journal of Medicine*, *373*(12), 1136-1152.

Dowding, J. M., Das, S., Kumar, A., Dosani, T., McCormack, R., Gupta, A., ... & Self, W. T. (2013). Cellular interaction and toxicity depend on physicochemical properties and surface modification of redox-active nanomaterials. *ACS Nano*, *7*(6), 4855-4868.

Dowding, J. M., Das, S., Kumar, A., Dosani, T., McCormack, R., Gupta, A., ... & Self, W. T. (2013). Cellular interaction and toxicity depend on physicochemical properties and surface modification of redox-active nanomaterials. *ACS Nano*, *7*(6), 4855-4868.

Durland-Busbice, S., & Reisman, D. (2002). Lack of p53 expression in human myeloid leukemias is not due to mutations in transcriptional regulatory regions of the gene. *Leukemia*, *16*(10), 2165.

Estevez, A. Y., & Erlichman, J. S. (2014). The potential of cerium oxide nanoparticles (nanoceria) for neurodegenerative disease therapy. *Nanomedicine*, *9*(10), 1437-1440.

Fadok, V. A., Bratton, D. L., Frasch, S. C., Warner, M. L., & Henson, P. M. (1998). The role of phosphatidylserine in recognition of apoptotic cells by phagocytes. *Cell Death and Differentiation*, *5*(7), 551.

Fadok, V. A., Savill, J. S., Haslett, C., Bratton, D. L., Doherty, D. E., Campbell, P. A., & Henson, P. M. (1992). Different populations of macrophages use either the vitronectin receptor or the phosphatidylserine receptor to recognize and remove apoptotic cells. *The Journal of Immunology*, *149*(12), 4029-4035.

Faraji, A. H., & Wipf, P. (2009). Nanoparticles in cellular drug delivery. *Bioorganic and Medicinal Chemistry*, *17*(8), 2950–2962.

Ferrara, F., & Schiffer, C. A. (2013). Acute myeloid leukaemia in adults. *The Lancet*, *381*(9865), 484-495.

Fulekar, M. H., Pathak, B., & Kale, R. K. (2014). Nanotechnology: perspective for environmental sustainability. In *Environment and Sustainable Development* Springer, New Delhi.pp. 87-114.

Ganzel, C., Manola, J., Douer, D., Rowe, J. M., Fernandez, H. F., Paietta, E. M., ... & Cripe, L. D. (2016). Extramedullary disease in adult acute myeloid leukemia is common but lacks independent significance: analysis of patients in ECOG-ACRIN cancer research group trials, 1980-2008. *Journal of Clinical Oncology*, *34*(29), 3544

Geary, C. G. (2000). The story of chronic myeloid leukaemia: Historical review. *British Journal of Haematology*, *110*(1), 2-11.

Gerke, V. (2002). Moss SE. *Annexins: from structure to function. Physiology Reviews*, *82*, 331-371.

Gerke, V. Ö. *Molecular Biology Letters*, *6*(2), 204-204.L. K. E. R. (2001). Annexins and membrane organisation in the endocytic pathway. *Cellular andMolecular BiologyLetters* 6 (2) 202-204.

Ghosh, S., & Hayden, M. S. (2012). Celebrating 25 years of NF- κB research. *Immunological Reviews*, *246*(1), 5-13.

Gianni, L., Herman, E. H., Lipshultz, S. E., Minotti, G., Sarvazyan, N., & Sawyer, D. B. (2008). Anthracycline cardiotoxicity: from bench to bedside. *Journal of Clinical Oncology: Official Journal of the American Society of Clinical Oncology*, *26*(22), 3777.

Golomb, H. M., Rowley, J. D., Vardiman, J. W., Testa, J. R., & Butler, A. (1980). " Microgranular" acute promyelocytic leukemia: a distinct clinical, ultrastructural, and cytogenetic entity. *Blood*, *55*(2), 253-259.

Grillo, R., Rosa, A. H., & Fraceto, L. F. (2015). Engineered nanoparticles and organic matter: a review of the state-of-the-art. *Chemosphere*, *119*, 608-619.

Haiss, W., Thanh, N. T. K., Aveyard, J., & Fernig, D. G. (2007). Determination of size and concentration of gold nanoparticles from UV-Vis spectra. *Analytical Chemistry*, *79*(11), 4215–4221.

Hande, K. R. (2008). Topoisomerase II inhibitors. *Update on Cancer Therapeutics*, *3*(1), 13-26.

Hassellov, M., Readman, J. W., Ranville, J. F., & Tiede, Æ. K. (2008). Nanoparticle analysis and characterization methodologies in environmental risk assessment of engineered nanoparticles. *Ecotoxicology*, 344–361.

He L, Gu J, Lim LY, Yuan Z X, Mo J (2016). Nanomedicine-mediated therapies to target breast cancer stem cells. *Frontiers in Pharmacology*, *7*, 313.

Herman, E. H., Zhang, J., Chadwick, D. P., & Ferrans, V. J. (2000). Comparison of the protective effects of amifostine and dexrazoxane against the toxicity of doxorubicin in spontaneously hypertensive rats. *Cancer chemotherapy and pharmacology*, *45*(4), 329-334.

Hoffmann, A., Natoli, G., & Ghosh, G. (2006). Transcriptional regulation via the NF-κB signaling module. *Oncogene*, *25*(51), 6706. Huang, J., Zhao, M., Li, X., Ma, L., Zhang, J., Shi, J., ... & Zhou, Y. (2015). The cytotoxic effect of the benzene metabolite hydroquinone is mediated by the modulation of MDR1 expression via the NF-κB signaling pathway. *Cellular Physiology and Biochemistry*, *37*(2), 592-602.

Injac, R., & Strukelj, B. (2008). Recent advances in protection against doxorubicin-induced toxicity. *Technology in Cancer Research &Treatment*, *7*(6), 497-516.

Jimmy, C. Y., Zhang, L., & Lin, J. (2003). Direct sonochemical preparation of high-surface-area nanoporous ceria and ceria–zirconia solid solutions. *Journal of Colloid and Interface Science*, *260*(1), 240-243.

Jin, M. W., Xu, S. M., An, Q., & Wang, P. (2016). A review of risk factors for childhood leukemia. *Eur Rev Med Pharmacol Sci*, *20*(18), 3760-3764.

Johnstone, R. W., Ruefli, A. A., & Lowe, S. W. (2002). Apoptosis: a link between cancer genetics and chemotherapy. *Cell*, *108*(2), 153-164.

Karin, M., Cao, Y., Greten, F. R., & Li, Z. W. (2002). NF-κB in cancer: from innocent bystander to major culprit. *Nature Reviews Cancer*, *2*(4), 301.

Kašpar, J., Fornasiero, P., & Graziani, M. (1999). Use of CeO2-based oxides in the three-way catalysis. *Catalysis Today*, *50*(2), 285-298

Kelly, L. M., & Gilliland, D. G. (2002). Genetics of myeloid leukemias. *Annual Review of Genomics and Human Genetics*, *3*(1), 179-198.

Kolachana, P., Subrahmanyam, V. V., Meyer, K. B., Zhang, L., & Smith, M. T. (1993). Benzene and its phenolic metabolites produce oxidative DNA damage in HL60 cells in vitro and in the bone marrow in vivo. *Cancer Research*, *53*(5), 1023-1026

Koopman, G., Reutelingsperger, C. P., Kuijten, G. A., Keehnen, R. M., Pals, S. T., & Van Oers, M. H. (1994). Annexin V for flow cytometric detection of phosphatidylserine expression on B cells undergoing apoptosis. *Blood*, *84*(5), 1415-1420.

Kumar, A., Das, S., Munusamy, P., Self, W., Baer, D. R., Sayle, D. C., & Seal, S. (2014). Behavior of nanoceria in biologically-relevant environments. *Environmental Science: Nano*, *1*(6), 516-532.

Larsen, A. K., Escargueil, A. E., & Skladanowski, A. (2003). Catalytic topoisomerase II inhibitors in cancer therapy. *Pharmacology &Therapeutics*, *99*(2), 167-181.

Lawrence, D., Shahrokh, Z., Marsters, S., Achilles, K., Shih, D., Mounho, B., ... & Hooley, J. (2001). Differential hepatocyte toxicity of recombinant Apo2L/TRAIL versions. *Nature Medicine*, *7*(4), 383.

Lee, S. J., Yum, Y. N., Kim, S. C., Kim, Y., Lim, J., Lee, W. J., ... & Sohn, S. (2013). Distinguishing between genotoxic and non-genotoxic hepatocarcinogens by gene expression profiling and bioinformatic pathway analysis. *Scientific Reports*, *3*, 2783.

Li, J., Jiang, S., Chen, Y., Ma, R., Chen, J., Qian, S., ... & Yu, K. (2018). Benzene metabolite hydroquinone induces apoptosis of bone marrow mononuclear cells through inhibition of β-catenin signaling. *Toxicology in Vitro*, *46*, 361-369.

Lin, Y., Xu, C., Ren, J., & Qu, X. (2012). Using Thermally Regenerable Cerium Oxide Nanoparticles in Biocomputing to Perform Label- free, Resettable, and Colorimetric Logic Operations. *Angewandte Chemie International Edition*, *51*(50), 12579-12583.

Lobatto, M. E., Fuster, V., Fayad, Z. A., & Mulder, W. J. (2011). Perspectives and opportunities for nanomedicine in the management of atherosclerosis. *Nature Reviews Drug Discovery*, *10*(11), 835.

Martin, S., Reutelingsperger, C. P., McGahon, A. J., Rader, J. A., Van Schie, R. C., LaFace, D. M., & Green, D. R. (1995). Early redistribution of plasma membrane phosphatidylserine is a general feature of apoptosis regardless of the initiating stimulus: inhibition by overexpression of Bcl-2 and Abl. *Journal of Experimental Medicine*, *182*(5), 1545-1556.

Meacham, C. E., & Morrison, S. J. (2013). Tumour heterogeneity and cancer cell plasticity. *Nature*, *501*(7467), 328.

Michael Jr, F. H. (2008). Nanominerals, mineral nanoparticles, and Earth system. *Science*, *319*, 1631.

Miller K. D, Siegel R. L, Lin C. C, Mariotto A. B, Kramer J. L, Rowland, J. H,& Jemal A (2016). Cancer treatment and survivorship statistics, 2016. *CA: ACancer Journal for Clinicians*, *66*(4), 271-289.

Minotti, G., Menna, P., Salvatorelli, E., Cairo, G., & Gianni, L. (2004). Anthracyclines: molecular advances and pharmacologic developments in antitumor activity and cardiotoxicity. *Pharmacological Reviews*, *56*(2), 185-229.

Mohanraj, V., Chen, Y., & Chen, M. &. (2006). Nanoparticles – A Review. *Tropical*

Journal of Pharmaceutical Research Trop J Pharm Res, *5*(June), 561–573.

Mori, N., Fujii, M., Ikeda, S., Yamada, Y., Tomonaga, M., Ballard, D. W., & Yamamoto, N. (1999). Constitutive activation of NF-κB in primary adult T-cell leukemia cells. *Blood*, *93*(7), 2360-2368.

Moss, L. A. S., Jensen-Taubman, S., & Stetler-Stevenson, W. G. (2012). Matrix metalloproteinases: changing roles in tumor progression and metastasis. *The American journal of pathology*, *181*(6), 1895-1899.

Mukhopadhyay, A., Bueso-Ramos, C., Chatterjee, D., Pantazis, P., & Aggarwal, B. B. (2001). Curcumin downregulates cell survival mechanisms in human prostate cancer cell lines. *Oncogene*, *20*(52), 7597.

Mussai, F., De Santo, C., Abu-Dayyeh, I., Booth, S., Quek, L., McEwen-Smith, R. M., ... Cerundolo, V. (2013). Acute myeloid leukemia creates an arginase-dependent immunosuppressive microenvironment. *Blood*, *122*(5), 749–758.

Nelson, B., Johnson, M., Walker, M., Riley, K., & Sims, C. (2016). Antioxidant cerium oxide nanoparticles in biology and medicine. *Antioxidants*, *5*(2), 15.

Octavia, Y., Tocchetti, C. G., Gabrielson, K. L., Janssens, S., Crijns, H. J., & Moens, A. L. (2012). Doxorubicin-induced cardiomyopathy: from molecular mechanisms to therapeutic strategies. *Journal of Molecular and Cellular Cardiology*, *52*(6), 1213-1225.

Oeckinghaus, A., & Ghosh, S. (2009). The NF-κB family of transcription factors and its regulation. *Cold Spring Harbor Perspectives in Biology*, *1*(4), a000034.

Patel, A. G., & Kaufmann, S. H. (2012). Cancer: How does doxorubicin work?. *Elife*, *1*, e00387.D'Azevedo, P. A., Tannhauser, M., Tannhauser, S. L., & Barros, H. M. (1996). Hematological alterations in rats from xylene and benzene. *Veterinary and Human Toxicology*, *38*(5), 340–4.

Patil, S., Kuiry, S. C., Seal, S., & Vanfleet, R. (2002). Synthesis of nanocrystalline ceria particles for high temperature oxidation resistant coating. *Journal of Nanoparticle Research*, *4*(5), 433-438.

Perez, J. M., Asati, A., Nath, S., & Kaittanis, C. (2008). Synthesis of biocompatible dextran- coated nanoceria with pH-dependent antioxidant properties. *Small*, *4*(5), 552-556.

Phillips, D. R., Greif, P. C., & Boston, R. C. (1988). Daunomycin-DNA dissociation kinetics. *Molecular Pharmacology*, *33*(2), 225-230.

Pirmohamed, T., Dowding, J. M., Singh, S., Wasserman, B., Heckert, E., Karakoti, A. S., ... & Self, W. T. (2010). Nanoceria exhibit redox state-dependent catalase mimetic activity. *Chemical Communications*, *46*(16), 2736-2738.

Pogorelcnik, B., Perdih, A., & Solmajer, T. (2013). Recent developments of DNA poisons-human DNA topoisomerase IIα inhibitors-as anticancer agents. *Current Pharmaceutical Design*, *19*(13), 2474-2488.

Prokocimer, M., Shaklai, M., Bassat, H. B., Wolf, D., Goldfinger, N., & Rotter, V. (1986). Expression of p53 in human leukemia and lymphoma. *Blood*, *68*(1), 113-118.

Priestman, T. (2012). *Cancer chemotherapy in clinical practice*. P.p 45-103, London : Springer Science & Business Media.

Qin, W., Huang G, Chen Z, & Zhang Y (2017). Nanomaterials in targeting cancer stem cells for cancer therapy. *Frontiers in Pharmacology*, *8*, 1.

Ramamurthy, C. H., Padma, M., mariya samadanam, I. D., Mareeswaran, R., Suyavaran, A., Kumar, M. S., ... Thirunavukkarasu, C. (2013). The extra cellular synthesis of gold and silver nanoparticles and their free radical scavenging and antibacterial properties. *Colloids and Surfaces B: Biointerfaces*, *102*, 808–815

Roy, H. (2016). Biochemical and histological alteration in rat kidney exposed to benzene leading to oxidative stress. *Journal of Cell and Tissue Research*, *16*(1), 5541-5545.

Sarmento, B., Ferreira, D., Veiga, F., & Ribeiro, A. (2006). Characterization of insulin-loaded alginate nanoparticles produced by ionotropic pre-gelation through DSC and FTIR studies. *Carbohydrate Polymers*, *66*(1), 1–7.

Sawyer, D. B. (2013). Anthracyclines and heart failure. *New England Journal of Medicine*, *368*(12), 1154-1156.

Siegel, R., Naishadham, D., & Jemal, A. (2013). Cancer statistics, 2013. *CA: ACancer Journal for Clinicians*, *63*(1), 11-30.

Singh, M., Singh, S., Prasad, S., & Gambhir, I. S. (2008). Nanotechnology in Medicine and Antibacterial Effect of. *Digest Journal of Nanomaterials and Biostructure*, *3*(3), 115–122.

Sinha, R., Kim, G. J., Nie, S., & Shin, D. M. (2006). Nanotechnology in cancer therapeutics: bioconjugated nanoparticles for drug delivery. *Molecular Cancer Therapeutics*, *5*(8), 1909–1917.

Sordet, O., Khan, Q. A., Kohn, K. W., & Pommier, Y. (2003). Apoptosis induced by topoisomerase inhibitors. *Current Medicinal Chemistry-Anti-Cancer Agents*, *3*(4), 271-290.

Spencer, S. L., & Sorger, P. K. (2011). Measuring and modeling apoptosis in single cells. *Cell*, *144*(6), 926-939.

Stuckey, D. W., & Shah, K. (2013). TRAIL on trial: preclinical advances in cancer therapy. *Trends in Molecular Medicine*, *19*(11), 685-694.

Sun, T., Zhang, Y. S., Pang, B., Hyun, D. C., Yang, M., & Xia, Y. (2014). Engineered nanoparticles for drug delivery in cancer therapy. *Angewandte Chemie International Edition*, *53*(46), 12320-12364.

Takemura, G., & Fujiwara, H. (2007). Doxorubicin-induced cardiomyopathy: from the cardiotoxic mechanisms to management. *Progress in Cardiovascular Diseases*, *49*(5), 330-352.

Thomas, B. J. C., Boccaccini, A. R., & Shaffer, M. S. P. (2005). Multi-walled carbon nanotube coatings using Electrophoretic Deposition (EPD). *Journal of the American Ceramic Society*, *88*(4), 980–982.

Tiwary, K. P., Choubey, S. K., & Sharma, K. (2013). Structural And Optical Properties OF ZnS Nanoparticles Synthesized By Microwave Irradiation Method.*Chalcogenide Letters,10*(9), 319–323

Torchilin, V. P. (2000). Drug targeting. *European Journal of Pharmaceutical Sciences*, *11*, S81-S91.

Vogelstein, B., & Kinzler, K. W. (2004). Cancer genes and the pathways they control. *Nature Medicine*, *10*(8), 789.

Wang, Q., Perez, J. M., & Webster, T. J. (2013). Inhibited growth of Pseudomonas aeruginosa by dextran-and polyacrylic acid-coated ceria nanoparticles. *International Journal of Nanomedicine*, *8*, 3395.

Wang, Y., Yang, F., Zhang, H. X., Zi, X. Y., Pan, X. H., Chen, F., ... & Hu, Y. P. (2013). Cuprous oxide nanoparticles inhibit the growth and metastasis of melanoma by targeting mitochondria. *Cell Death &Disease*, *4*(8), e783.

Waris, G., & Ahsan, H. (2006). Reactive oxygen species: role in the development of cancer and various chronic conditions. *Journal of Carcinogenesis*, *5*, 14.

Wason, M. S., Colon, J., Das, S., Seal, S., Turkson, J., Zhao, J., & Baker, C. H. (2013). Sensitization of pancreatic cancer cells to radiation by cerium oxide nanoparticle-induced ROS production. *Nanomedicine: Nanotechnology, Biology and Medicine*, *9*(4), 558-569.

Weiss, R. B. (1992, December). The anthracyclines: will we ever find a better doxorubicin?. In *Seminars in oncology* (Vol. 19, No. 6, pp. 670-686).

Wicki, A., Witzigmann, D., Balasubramanian, V., & Huwyler, J. (2015). Nanomedicine in cancer therapy: challenges, opportunities, and clinical applications. *Journal of Controlled Release*, *200*, 138-157

Wilstermann, A. M., & Osheroff, N. (2003). Stabilization of eukaryotic topoisomerase II-DNA cleavage complexes. *Current Topics in Medicinal Chemistry*, *3*(3), 321-338.

Xu, C., & Qu, X. (2014). Cerium oxide nanoparticle: a remarkably versatile rare earth nanomaterial for biological applications. *NPG Asia Materials*, *6*(3), e90.

Xu, C., Lin, Y., Wang, J., Wu, L., Wei, W., Ren, J., & Qu, X. (2013). Nanoceria- Triggered Synergetic Drug Release Based on CeO2- Capped Mesoporous Silica Host–Guest Interactions and Switchable Enzymatic Activity and Cellular Effects of CeO2. *Advanced Healthcare Materials*, *2*(12), 1591-1599.

Xu, L., Liu, J., Chen, Y., Yun, L., Chen, S., Zhou, K., ... & Tang, H. (2017). Inhibition of autophagy enhances Hydroquinone-induced TK6 cell death. *Toxicology in Vitro*, *41*, 123-132.

Zhang L Q, Lv R W, Qu X. D, Chen X J, Lu HS, & Wang Y (2017). Aloesin suppresses cell growth and metastasis in ovarian cancer SKOV3 cells through the inhibition of the MAPK signaling pathway. *Analytical Cellular Pathology, 2017.*

turnitin

Digital Receipt

This receipt acknowledges that Turnitin received your paper. Below you will find the receipt information regarding your submission.

The first page of your submissions is displayed below.

Submission author:	Asiya Esa
Assignment title:	plagiarism
Submission title:	plagiarism report-thesis
File name:	plagiarism_check.pdf
File size:	1.82M
Page count:	73
Word count:	12,543
Character count:	67,016
Submission date:	04-Jul-2019 10:09AM (UTC+0500)
Submission ID:	1149140359

Exploration of Molecular Machinery Affected by Cerium Oxide Nanoparticles in Benzene Induced Leukemia

by

Asiya Esa

Department of Biochemistry
Faculty of Biological Sciences
Quaid-i-Azam University
Islamabad, Pakistan

2019

Clarein

plagiarism report-thesis

ORIGINALITY REPORT

15%	6%	6%	13%
SIMILARITY INDEX	INTERNET SOURCES	PUBLICATIONS	STUDENT PAPERS

PRIMARY SOURCES

1	Submitted to Higher Education Commission Pakistan Student Paper	2%
2	Submitted to National University of Singapore Student Paper	1%
3	Submitted to Universiti Malaysia Terengganu UMT Student Paper	<1%
4	Al-Amoudi , Wafa Abdullah Mosa. "Antioxidant Activity of Anticancer Chromium and Cobalt Complexes of Bromobenzaldehyde-Iminacetophenone against Ehrlich Ascites Carcinoma Cells Induced in Mice = النشاط المضاد للأكسدة لمتراكبات الكروم والكوبالت لبروموبنزألدهيد - ايمين الأسيتوفينون المضادة للسرطان ضد خلايا إيرلخ السرطانية المستحدثة في الفئران", King Abdulaziz University : Scientific Publishing Centre, 2017 Publication	<1%
5	Submitted to Universiti Sains Malaysia Student Paper	<1%